





# A Conserved Streptococcal Virulence Regulator Controls the Expression of a Distinct Class of M-Like Proteins

Jonathan D. D’Gama,<sup>a,b</sup> Zhe Ma,<sup>b,c,d,e</sup> Hailong Zhang,<sup>a,b</sup> Xu Liu,<sup>a,b</sup>  Hongjie Fan,<sup>c,d,e</sup> Ellen Ruth A. Morris,<sup>f</sup>  Noah D. Cohen,<sup>f</sup> Colette Cywes-Bentley,<sup>a,b</sup> Gerald B. Pier,<sup>a,b</sup> Matthew K. Waldor<sup>a,b,g</sup>

<sup>a</sup>Department of Microbiology, Harvard Medical School, Boston, Massachusetts, USA

<sup>b</sup>Division of Infectious Diseases, Brigham and Women’s Hospital, Boston, Massachusetts, USA

<sup>c</sup>MOE Joint International Research Laboratory of Animal Health and Food Safety, College of Veterinary Medicine, Nanjing Agricultural University, Nanjing, Jiangsu, China

<sup>d</sup>Ministry of Agriculture Key Laboratory of Animal Bacteriology, Nanjing, Jiangsu, China

<sup>e</sup>Jiangsu Co-Innovation Center for Prevention and Control of Important Animal Infectious Diseases and Zoonoses, Yangzhou, Jiangsu, China

<sup>f</sup>Department of Large Animal Clinical Sciences, College of Veterinary Medicine and Biomedical Sciences, College Station, Texas, USA

<sup>g</sup>Howard Hughes Medical Institute, Boston, Massachusetts, USA

**ABSTRACT** *Streptococcus equi* subspecies *zooepidemicus* (SEZ) are group C streptococci that are important pathogens of economically valuable animals such as horses and pigs. Here, we found that many SEZ isolates bind to a monoclonal antibody that recognizes poly-*N*-acetylglucosamine (PNAG), a polymer that is found as a surface capsule-like structure on diverse microbes. A fluorescence-activated cell sorting-based transposon insertion sequencing (Tn-seq) screen, coupled with whole-genome sequencing, was used to search for genes for PNAG biosynthesis. Surprisingly, mutations in a gene encoding an M-like protein, *szM*, and the adjacent transcription factor, designated *sezV*, rendered strains PNAG negative. *SezV* was required for *szM* expression and transcriptome analysis showed that *SezV* has a small regulon. SEZ strains with inactivating mutations in either *sezV* or *szM* were highly attenuated in a mouse model of infection. Comparative genomic analyses revealed that linked *sezV* and *szM* homologues are present in all SEZ, *S. equi* subspecies *equi* (SEE), and M18 group A streptococcal (GAS) genomes in the database, but not in other streptococci. The antibody to PNAG bound to a wide range of SEZ, SEE, and M18 GAS strains. Immunochemical studies suggest that the SzM protein may be decorated with a PNAG-like oligosaccharide although an intact oligosaccharide substituent could not be isolated. Collectively, our findings suggest that the *szM* and *sezV* loci define a subtype of virulent streptococci and that an antibody to PNAG may have therapeutic applications in animal and human diseases caused by streptococci bearing SzM-like proteins.

**IMPORTANCE** M proteins are surface-anchored virulence factors in group A streptococci, human pathogens. Here, we identified an M-like protein, SzM, and its positive regulator, *SezV*, in *Streptococcus equi* subspecies *zooepidemicus* (SEZ), an important group of pathogens for domesticated animals, including horses and pigs. SzM and *SezV* homologues were found in the genomes of all SEZ and *S. equi* subspecies *equi* and M18 group A streptococcal strains analyzed but not in other streptococci. Mutant SEZ strains lacking either *sezV* or *szM* were highly attenuated in a mouse model of infection. Collectively, our findings suggest that *SezV*-related regulators and the linked SzM family of M-like proteins define a new subset of virulent streptococci.

**KEYWORDS** M protein, *Streptococcus equi*, *Streptococcus zooepidemicus*, whole-genome sequencing, group A streptococcus, streptococcal pathogenesis, virulence regulation

**Citation** D’Gama JD, Ma Z, Zhang H, Liu X, Fan H, Morris ERA, Cohen ND, Cywes-Bentley C, Pier GB, Waldor MK. 2019. A conserved streptococcal virulence regulator controls the expression of a distinct class of M-like proteins. *mBio* 10:e02500-19. <https://doi.org/10.1128/mBio.02500-19>.

**Editor** Michael S. Gilmore, Harvard Medical School

**Copyright** © 2019 D’Gama et al. This is an open-access article distributed under the terms of the [Creative Commons Attribution 4.0 International license](https://creativecommons.org/licenses/by/4.0/).

Address correspondence to Zhe Ma, [mazhe@njau.edu.cn](mailto:mazhe@njau.edu.cn).

J.D.D’G. and Z.M. contributed equally to this article.

This article is a direct contribution from Gerald B. Pier, a Fellow of the American Academy of Microbiology, who arranged for and secured reviews by Michael Wessels, Boston Children’s Hospital, and Andrew Waller, Animal Health Trust.

**Received** 19 September 2019

**Accepted** 23 September 2019

**Published** 22 October 2019

*Streptococcus equi* subspecies *zoepidemicus* (SEZ) is a Lancefield group C streptococcus (GCS) that is a constituent of the normal upper respiratory tract flora of domesticated animals, such as horses (1). SEZ is also an opportunistic pathogen, and infections in a wide range of animals, including pigs, cows, dogs, and horses, have been reported (1, 2). Epizootic outbreaks in livestock (e.g., swine in China) can be widespread and severe, resulting in significant economic loss (3, 4). Infection of horses with another *S. equi* biovar, *S. equi* subspecies *equi* (SEE), causes the severe, contagious respiratory infection known as strangles (5). SEZ infection of humans, who typically acquire the pathogen through contact with infected animals or contaminated milk or cheese, typically causes meningitis and can be fatal (6, 7). Several virulence factors and protective antigens have been identified in SEZ/SEE, including two M-like proteins, referred to as SzM/SeM and SzP/SzPSe (8–10).

The M/M-like protein family is a class of surface-associated streptococcal proteins that includes M protein, a classical virulence factor of group A streptococcus (GAS; *S. pyogenes*) (11). Proteins in the group are anchored to the cell wall, share several features (including a primarily alpha-helical/coiled-coil structure, a polar cytoplasmic C-terminal tail, and an extracellular distal N terminus), and function in modulating the host immune response to the pathogen. The diverse immunomodulatory functions of M/M-like proteins include but are not limited to fibrinogen binding, inhibition of complement activation, antiphagocytic activity, and binding to Fc portions of immunoglobulins (11, 12). M/M-like proteins are typically key streptococcal virulence factors that can be targets of protective antibody responses (11–13). The flexible set of criteria for M/M-like protein classification has led to ambiguity in the field since various types of M-like proteins have different designations, functions, and sequences (11).

The SzM M-like protein in SEZ has been shown to bind fibrinogen, activate plasminogen, inhibit phagocytosis, and serve as a protective antigen for vaccination (9, 14). However, the contribution of SzM to SEZ virulence *in vivo* has not been determined. SzP, a second SEZ M-like protein, has been shown to contribute to SEZ virulence in an animal model (8, 15). An SzM ortholog in SEE, SeM (also called FgBP [16]), has also been shown to be an important virulence factor when evaluated in mice (16, 17). Dale et al. (18) noted that certain strains of GAS, particularly of the M18 type, encode a SzM ortholog, called Spa (streptococcal protective antigen), which is linked to virulence (19). In the M18 strain studied, a Spa deletion mutant was more attenuated in mice than a mutant with the canonical M18 protein deleted and Spa was a protective antigen as well (19). Although homologs of SzM have been found in several SEZ, SEE, and GAS strains, the distribution and extent of conservation of SzM homologs in strains of these species and in other streptococcal species is unknown. Furthermore, factors governing the expression of SzM or its homologs have not been described. In contrast, the regulation of M protein and two classes of M-like proteins (M-related protein [Mrp] and M-like protein [Enn]) in GAS by the central virulence regulator, Mga (multiple gene activator), is well described (11, 20, 21).

In addition to M/M-like proteins, capsular polysaccharides and other surface polysaccharides are also important streptococcal virulence factors and protective antigens (22–26). For example, the GAS carbohydrate is critical for GAS virulence (22, 23). Poly-*N*-acetyl-*D*-glucosamine (PNAG) is a surface polysaccharide found on numerous Gram-positive and -negative bacteria and fungi (27, 28) that can serve as a virulence factor and a protective antigen (27, 28). Surface PNAG has been identified in *S. pneumoniae*, *S. pyogenes*, and *S. dysgalactiae* (27), but the loci encoding PNAG biosynthesis have not been described in streptococci. Also, the chemical bases of the association of PNAG with the microbial surface have not been elucidated, and it is unknown whether PNAG is physically linked to the cell membrane or cell wall.

Here, we found that SEZ is bound by a monoclonal antibody to PNAG and performed a fluorescence-activated cell sorting (FACS)-based transposon-insertion sequencing (Tn-seq) screen to identify genes required for surface production of PNAG by SEZ. Unexpectedly, the screen identified SzM and a conserved adjacent locus (termed here *SezV* for SEZ virulence) that promotes *szM* expression. An anti-PNAG monoclonal

antibody was found to directly interact with SzM, suggesting that this M-like protein may be decorated with a PNAG-like glycan. SEZ mutants lacking either *sezV* or *szM* were highly attenuated in a mouse model of infection. Comparative genomics revealed that *szM*, *seM*, and/or *spa* (here referred to as *szM/seM/spa*) are linked to *sezV* in all SEZ and SEE strains in the database, as well as in all M18 GAS, but not in other streptococci. Thus, our findings suggest that *SezV*-related regulators and the linked SzM family of M-like proteins define a new subset of virulent streptococci.

## RESULTS

**Tn-seq screen for loci required for surface PNAG expression.** We observed that a porcine SEZ isolate (ATCC 35246) (referred to as SEZ) was bound by a human anti-PNAG monoclonal antibody (MAb F598) (Fig. 1A), and we set out to identify loci that contribute to PNAG synthesis in SEZ. First, we developed a flow cytometry-based system for high-throughput analysis of the PNAG phenotype of single bacteria, using fluorescently conjugated F598 (AF488-F598). There was a considerable range of fluorescence intensities among a population of AF598 bound stationary-phase cells, but this range had minimal overlap with that of cells bound by an AF488-labeled isotype control antibody (F429) (Fig. 1A). Notably, although F429 was raised against an unrelated carbohydrate, it was engineered to include IgG1 heavy- and light-chain constant region amino acid sequences identical to those of F598 (29). Fluorescence microscopy using these two labeled antibodies confirmed that F598, but not F429, bound to SEZ cells (Fig. 1A), consistent with the idea that SEZ expresses surface PNAG.

To generate a genetically heterogeneous population of SEZ containing easily mappable mutations, we developed a method to generate a complex transposon-insertion (Tn) library in SEZ. Using the recently developed pMar4s mariner-based transposon delivery vector (30), a library containing transposons in >50% of potential insertion sites was created (see Fig. S1A and B in the supplemental material). A FACS-based screen of the Tn library with several rounds of selection for bacteria with low fluorescent intensity after staining with AF598 was carried out (Fig. 1B and C). We performed the screen with outgrowth in either liquid (screen A) or solid (screen B) media; more modest gating thresholds were applied in the latter, with the aim of identifying genes with weaker phenotypes. Despite the low (background) fluorescence intensity of all bacterial cells after the final rounds of selection (Fig. 1C), Tn-seq of the selected libraries revealed few genes (screen A, 2; screen B, 16; with average TA sites hit in the input of  $\geq 5$ ,  $\log_2$ -fold changes [L2FC] of  $\geq 2$ , an  $P \leq 0.05$ ) with statistically significant increased ratios of insertions (fold change values) in the sorted versus the input population (Fig. 1D; see Table S1 in the supplemental material). Notably, after the final round of selection in screen A, there was marked enrichment of only a single Tn insertion (in RS01795; Fig. 1D), suggesting that a jackpot event occurred at some point in the screen. Single gene deletions in two of the top hits (RS01795, [WP\\_014622330.1](#), L2FC = 6.8,  $1/P = 3.3$ ; and RS00930, [WP\\_014622184.1](#), L2FC = 4.9,  $1/P = 416.2$ ) were created, but neither lost MAb F598 binding (Fig. S1C). A second independently generated  $\Delta$ RS00930 gene deletion strain lacked MAb F589 binding (Fig. S1C), but complementation with RS00930 did not restore F598 binding, suggesting that RS00930 is not required for F598 binding. The preservation of F598 binding in the single gene deletion mutants suggested that the Tn insertions did not account for the absence of F598 binding in the screen hits.

Whole-genome sequencing (WGS) was used to identify mutations that were shared by SEZ mutants deficient in F598 binding. Several strains were sequenced, including a few Tn mutants and the RS00930 gene deletion strain that lacked F598 binding. Comparative analyses of these genome sequences revealed that 4 out of 5 F598 negative strains contained one of three distinct mutations in a single gene, RS09465 ([WP\\_038674722.1](#), old locus tag *SeseC\_02416*), which we have termed *sezV* (for SEZ virulence, Fig. 1E and F). The amino acid sequence of *SezV* is predicted to contain two domains, an N-terminal sensor kinase-like domain and an AraC helix-turn-helix (HTH) DNA-binding domain, suggesting that the protein is a transcriptional regulator. The

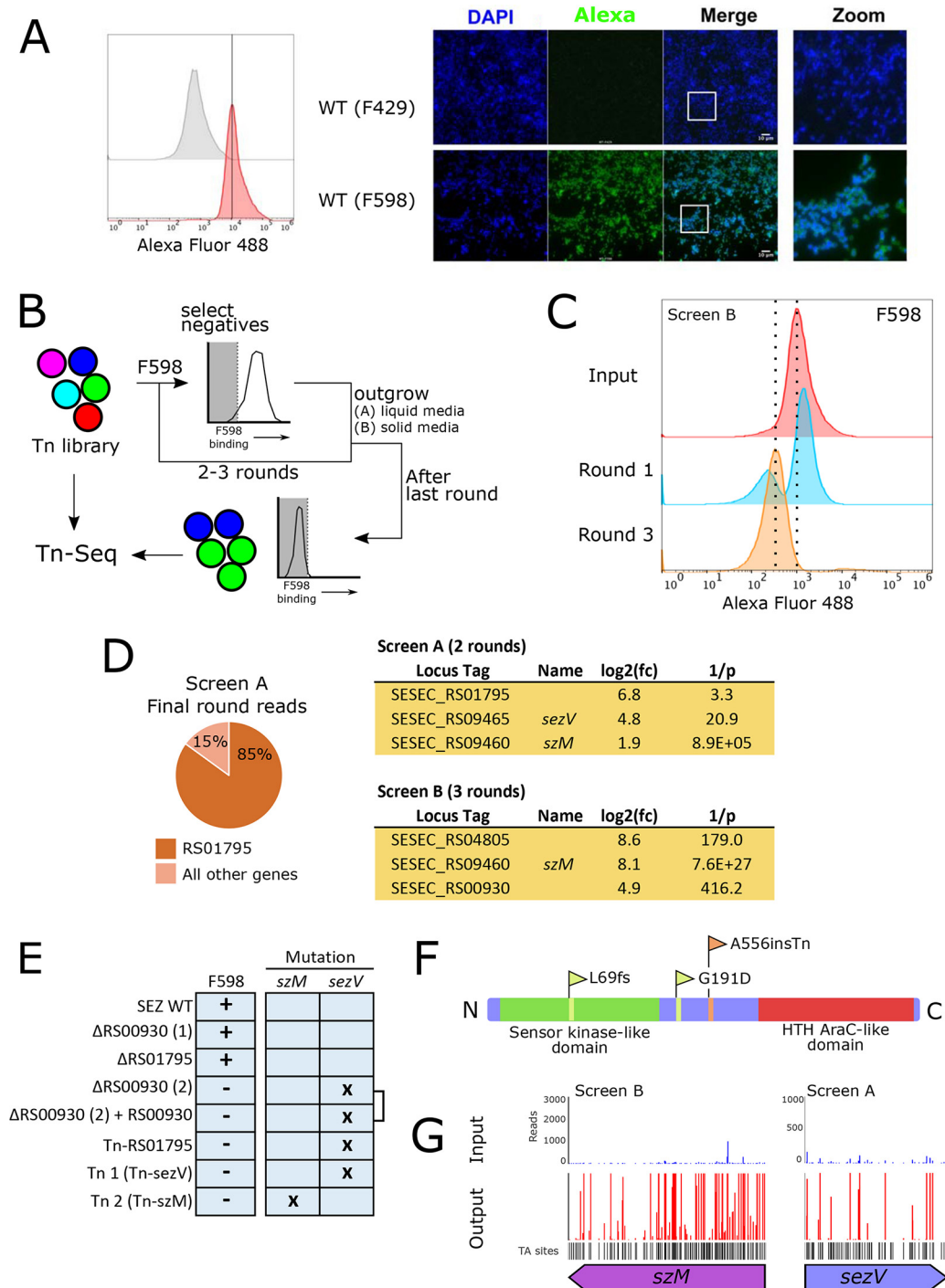


**FIG 1** Tn-seq and WGS screens for identification of loci required for surface PNAG expression in SEZ. (A, left) Flow cytometry of SEZ stained with an AF488-conjugated MAb to alginate (F429, negative control) or PNAG (F598). (Right) Microscopy of SEZ stained with DAPI and either AF488-F429 or AF488-F598. The white scale bar represents 10  $\mu$ m. (B) Schematic for Tn-seq screen for genes required for expression of surface PNAG. (C) AF488-F598 (anti-PNAG) binding to SEZ Tn library at different stages of the Tn-seq screen. Flow cytometry data are taken from screen B. Round 1, after first round of selection; round 3, after third round of selection. Dotted lines are included to help guide the eye. (D, left) Pie chart of the percentage of all reads mapping to a single site in gene RS01795 in the last round of screen A. (Right) Table of selected potential candidate genes required for PNAG expression from Tn-seq screen. (E) AF488-F598 binding phenotype and gene mutated based on WGS of indicated strains. The bracket indicates that strain  $\Delta$ RS00930 + RS00930 (2), which was derived from strain  $\Delta$ RS00930 (2), has the exact same mutation in *sezV* as is found in  $\Delta$ RS00930 (2). Tn1 contained a transposon insertion in *sezV*; Tn2 contained a transposon insertion in *szM*. (F) Location of mutants and domain organization of *sezV*. HTH, helix-turn-helix. Domains in *SezV* were predicted using HHpred (65, 68) and Phyre2 (69). (G) Comparison of the read count distributions of transposon insertions in *szM* and *sezV* in the input library and in the last round of the screen reveals uniform enrichment of insertions across these genes.

remaining F598 negative strain sequenced contained a mutation in the gene coding SzM (RS09460, [WP\\_014623570.1](#), old locus tag SeseC\_02415), a gene adjacent to and divergently transcribed from *sezV* (Fig. 1E and G). None of the three F598-positive strains sequenced contained a mutation in either *sezV* or *szM*. Furthermore, Tn insertions in both *sezV* and *szM* were hits in the Tn-seq screens (Fig. 1D and G), suggesting that these linked loci play roles in presentation of PNAG related epitopes in SEZ and thus facilitate F598 binding.

**Phenotypic characterization of strains lacking *sezV* or *szM*.** A  $\Delta$ *sezV* mutant was created, and this strain did not bind AF488-F598 either in flow cytometry or fluorescence microscopy (Fig. 2A and B). Complementation with *sezV* restored the F598 binding activity, establishing that this putative transcription factor is required for binding of this anti-PNAG MAbs. We were unable to construct a  $\Delta$ *szM* mutant, but we found that complementation of the Tn-*szM* mutant (a strain isolated with a transposon insertion in *szM*) with *szM* restored F598 binding activity (Fig. 2A and B).

Transmission electron microscopy (TEM) and scanning electron microscopy (SEM) were used to compare the surfaces of wild-type (WT),  $\Delta$ *sezV*, and Tn-*szM* mutant cells. In TEM, the  $\Delta$ *sezV* and Tn-*szM* mutants had smoother outer surfaces than the WT, complemented, and  $\Delta$ *hasB* strains, which does not produce the SEZ hyaluronic acid capsule (31) (Fig. 2C). The surface structures in the WT,  $\Delta$ *sezV* complemented, and  $\Delta$ *hasB* strains resemble the electron-dense surface “fuzzy coat” attributable to M protein fibers on the surfaces of GAS (32, 33). In SEM, the surfaces of the  $\Delta$ *sezV* and Tn-*szM* mutants also appeared smoother than the other strains (Fig. 2D). Together, these observations suggest that *sezV* and *szM* are required for the production of a major surface associated component in SEZ.

***sezV* activates the expression of *szM*.** The expression of M/M-like proteins in GAS is activated by *mga*, a gene that is generally found upstream of and transcribed in the same direction as the gene encoding the M/M-like protein. However, no regulator of *szM* (also known as *seM/fgbp* or *spa*) has been described. Although *sezV* bears no similarity to *mga*, its predicted domain architecture suggests that it is a transcriptional regulator (Fig. 1F) and the *sezV* gene is adjacent to the *szM* gene in the SEZ genome (Fig. 3A). Quantitative reverse transcription-PCR (RT-PCR) showed that there were reduced levels of *szM* transcripts in the  $\Delta$ *sezV* background, and this deficiency was complemented by exogenous *SezV*, strongly suggesting that *sezV* promotes *szM* expression (Fig. 3A). The transcriptomes of the WT and  $\Delta$ *sezV* strains were compared to identify other loci regulated by *sezV* (Fig. 3B and C; Table S1). This comparison revealed that *sezV* has a relatively small regulon; only one gene, *szM*, had expression reduced >5-fold in the mutant background, and only three genes, all within a fimbrial operon encoding a Fim1 pilus that includes a *cne* (collagen-binding protein of *S. equi*) homolog (34, 35), had expression increased >10-fold in the absence of *sezV*. Expression of the gene encoding SzP, the other M-like protein in SEZ, was largely unaffected in the absence of *sezV* ( $\log_2$ -fold change of 0.8; WT/ $\Delta$ *sezV*). Thus, *sezV* appears to primarily activate expression of *szM* and repress expression of a Fim1 pilus locus that encodes a *cne* homolog; notably, *Cne* has been explored as a candidate component of a vaccine for SEE (36–38).

***sezV* and *szM* both contribute to SEZ virulence.** A murine model of SEZ virulence (39) was used to test whether *sezV* or *szM* contribute to SEZ pathogenicity. In this model, intravenous (i.v.) inoculation of female adult C57B6/J mice with WT SEZ results in 100% mortality by 48 h postinfection (hpi) (Fig. 3D). The  $\Delta$ *sezV* strain was highly attenuated and exhibited both delayed kinetics of mortality (0% death at 48 hpi) and diminished absolute lethality (30% dead 1 week after infection). Plasmid-based complementation of the  $\Delta$ *sezV* mutant largely restored virulence, indicating that *sezV* is a key regulator of SEZ virulence. The Tn-*szM* mutant was also attenuated in this model, revealing that *szM* contributes to SEZ pathogenicity. There was no difference between the Kaplan-Meier curves for the  $\Delta$ *sezV* and Tn-*szM* mutants, raising the possibility that the virulence defect of the *sezV* mutant is largely explained by defective *szM* expression

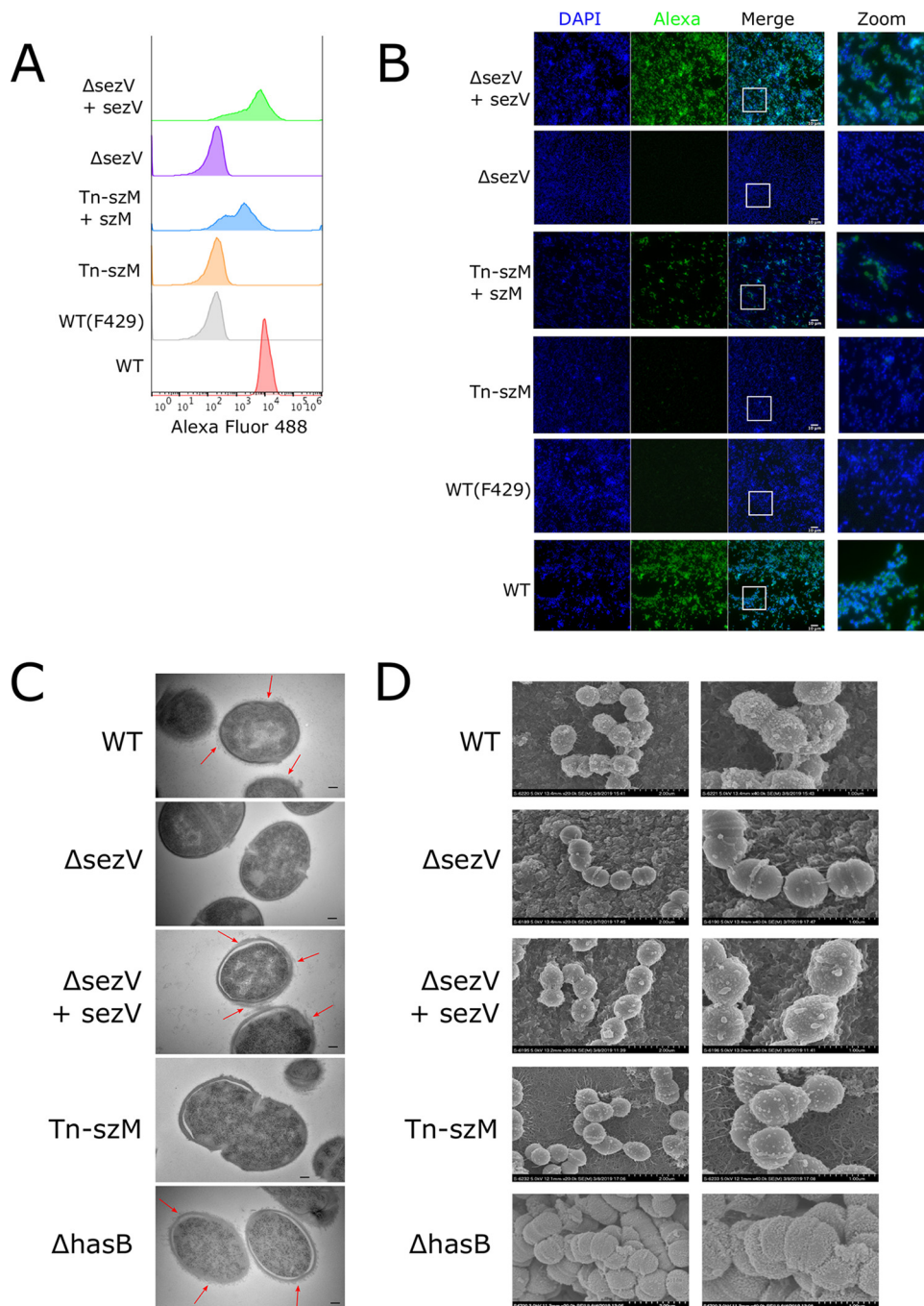


**FIG 2** Inactivation of *sezV* or *szM* leads to loss of SEZ reactivity with anti-PNAG antibody and to reduction in surface material. (A) Flow cytometry of indicated strains with AF488-F598. The WT strain was also stained with the negative-control antibody AF488-F429. (B) Microscopy of SEZ strains stained with DAPI and AF488-F598. The WT strain was also stained with AF488-F429. The rightmost panels provide zoomed views of the merged images. The white scale bar represents 10  $\mu$ m. (C) TEM images of SEZ strains. Red arrows indicate the surface material present on select strains. The black scale bar represents 500 nm. (D) SEM images of the indicated SEZ strains at lower (20K, left) and higher (40K, right) resolutions.

in this strain. In addition, the WT,  $\Delta$ sezV, and Tn-szM mutant strains grew similarly in culture, suggesting that the attenuation of the mutant strains is not due to growth defects caused by these mutations (Fig. S2A).

Given the rapid mortality induced by the WT SEZ strain, organs were collected 24 hpi to measure the bacterial burdens of the four strains in infected host tissues. As

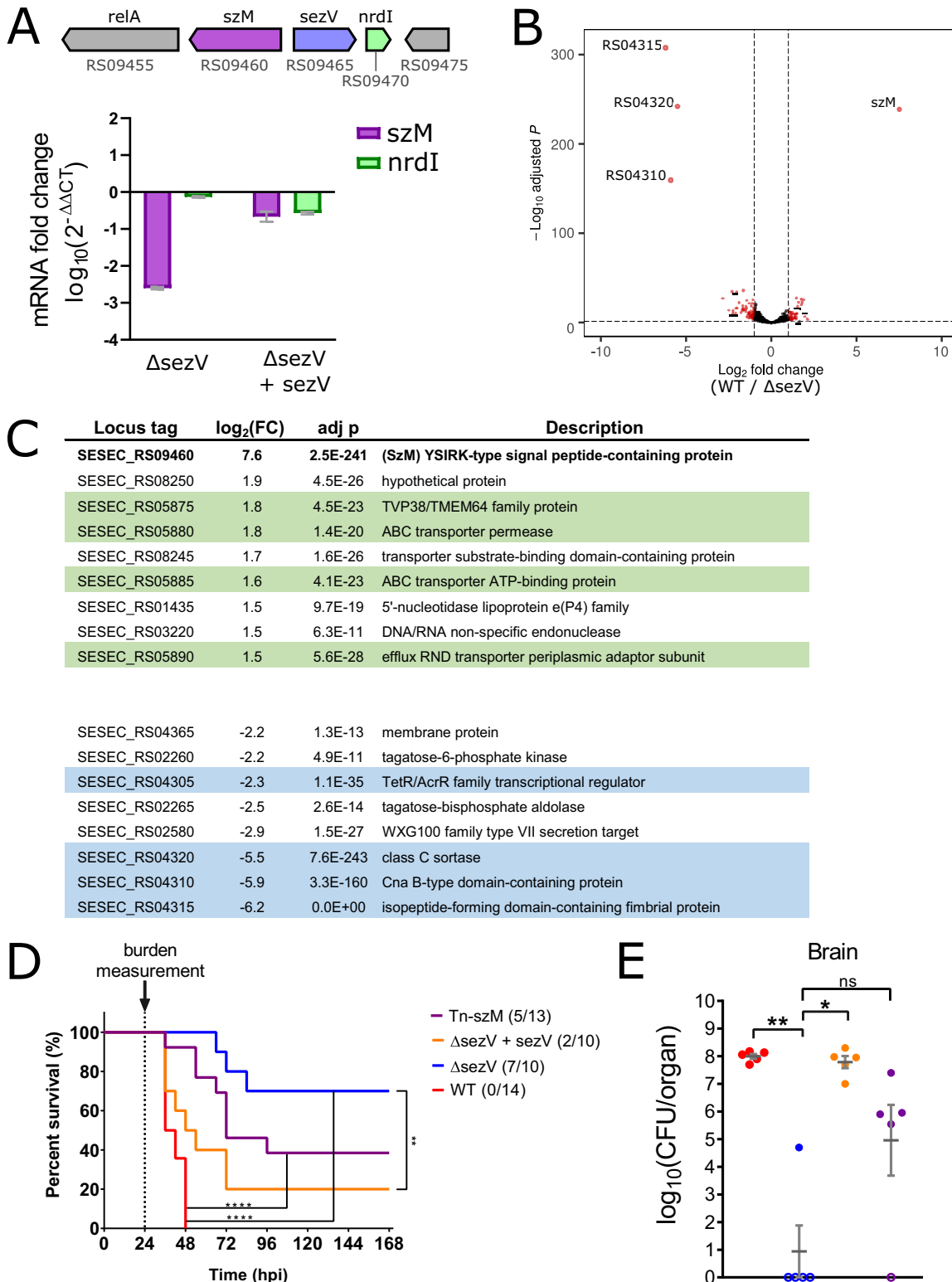


**FIG 3** *sezV* is required for expression of *szM* and SEZ virulence. (A, top) Genomic context of *szM* (RS09460) and *sezV* (RS09465) loci in the SEZ ATCC 35246 genome. (Bottom) Relative expression of *szM* and *nrdI* in the  $\Delta$ *sezV* and  $\Delta$ *sezV* complemented ( $\Delta$ *sezV* + *sezV*) strains compared to the WT strain. (B) Volcano plot of RNA-seq results comparing WT and  $\Delta$ *sezV* strains. The most differentially expressed genes, *szM* and the three genes from the same fimbriae operon (the *cne* homolog-containing Fim1 pilus locus), are labeled. Genes whose expression requires *sezV* have a positive fold change. (C) RNA-seq data for a selected set of genes that includes those with the highest log<sub>2</sub>-fold change [ $\log_2(\text{FC})$ ; WT/ $\Delta$ *sezV*]. The adjusted *P* value (adj *p*) from DESeq2 is shown. Genes found in gene clusters or operons are highlighted in the same color. The full list of genes is found in Table S1. (D) Kaplan-Meier survival curves of mice i.v. inoculated with the indicated SEZ strains. Curves were compared using the log-rank (Mantel-Cox) test. Numbers in parentheses refer to animals that died and

(Continued on next page)

observed previously, the highest burden of the WT SEZ strain was found in the brain, reflecting the neurotropism of this pathogen (39). Strikingly, in most mice, no  $\Delta$ sezV CFU were recovered from the brains of infected mice, and this marked virulence defect was corrected by genetic complementation (Fig. 3E). The burden of the  $\Delta$ sezV mutant in the blood and other organs was also reduced compared to the WT strain (Fig. S2B to F), but the magnitude of the defect was not as pronounced as observed in the brain. The burden of the Tn-szM mutant in the brain was also reduced, but not as dramatically as the  $\Delta$ sezV mutant; however, the burden of these two mutants was similarly reduced in other organs (Fig. 3E; Fig. S2B to F).

**MAB to PNAG binds SzM.** Our observations that the Tn-szM mutant was not recognized by MAb F598 in either flow cytometry or by fluorescence microscopy (Fig. 2) and that F598 binding was restored by expression of szM strongly suggest that surface presentation of SzM and PNAG are linked. Immunoblots confirmed this linkage. In Western blots of lysates from WT SEZ, a band of ~60 kDa, which is slightly greater than the predicted molecular weight of the mature form of SzM (~57 kDa, after N- and C-terminal processing) was detected with the F598 MAb to PNAG (Fig. 4A). This band was not detected in lysates derived from strains with the transposon insertion in szM (Tn-szM) or the deletion of sezV, but it was restored by complementation of the respective mutations (Fig. 4A). Moreover, a band of apparently the same molecular weight was observed in the same lysates (run on the same SDS-PAGE gel) when antisera raised against the recombinant SEE M-like SeM protein (anti-SeM sera) were used (Fig. 4A). When the blots were probed with MAb F429, an isotype control that was used at the same concentration as F598, bands were not detectable, though they became faintly detectable with longer exposure times (Fig. S3A). Together, these observations suggest the possibility that SzM is decorated by some form of PNAG. However, PNAG is ordinarily an extended capsule-like polymer that barely enters polyacrylamide gels such as the purified material used in Fig. 4A (and Fig. S3B).

To confirm that the antibody to PNAG and the antibody to M-protein bound to the same protein, SzM was purified using anti-SeM sera; no protein was purified from lysates of Tn-szM using the same protocol (Fig. S3C). The purified protein was bound by F598, as well as by anti-SeM (Fig. 4B). Mass spectrometry analysis of the peptides produced by trypsin digestion of the protein immunoprecipitated with the anti-SeM antisera confirmed that it was SzM; peptides were detected that span the majority of the predicted processed form of the protein (i.e., lacking the signal sequence and extreme C terminus, which is presumably cleaved as a result of sortase-mediated attachment of SzM to the cell wall) (Fig. S3D). Together, these observations establish that the MAb F598 to PNAG binds to SzM. F598 also bound to a single band recognized by anti-SeM in lysates of SEE strain CDL (Fig. 4C), suggesting that a PNAG-like molecule may decorate SzM homologs in other species.

To further investigate the chemical bases of the epitopes of SzM and SeM bound by F598, lysates of SEZ and SEE were treated with sodium periodate. This reagent opens the rings between vicinal hydroxyl groups generating aldehydes and is known to disrupt the structure of PNAG such that it is no longer recognized by F598 (27) (Fig. 4C). Periodate-treated bacterial lysates of SEZ and SEE were no longer bound by F598 but retained anti-SeM binding; however, the molecular weights of the proteins recognized by the anti SeM antisera shifted to slower-migrating forms, suggesting that the periodate treatment may have led to the formation of higher-order oligomers of SzM and SeM (Fig. 4C). These lysates were also treated with dispersin B, an enzyme that specifically cleaves the  $\beta$ -1,6 linkage between glucosamines in PNAG (40). After prolonged treatment with this enzyme, there was a marked reduction in F598 binding with

### FIG 3 Legend (Continued)

total animals inoculated (\*\*\*\*,  $P < 0.0001$ ; \*\*,  $P < 0.001$ ; \*,  $P < 0.05$ ). Comparisons that are nonsignificant are not labeled. (E) SEZ burdens recovered from brains of infected animals at 24 h postinfection. Colors of strains are the same as in panel D. Open circles represent animals for which no CFU were recovered. Groups were compared using a Kruskal-Wallis test with Dunn's multiple-comparison test (\*\*\*\*,  $P < 0.0001$ ; \*\*,  $P < 0.001$ ; \*,  $P < 0.05$ ). Comparisons that are nonsignificant are not labeled.



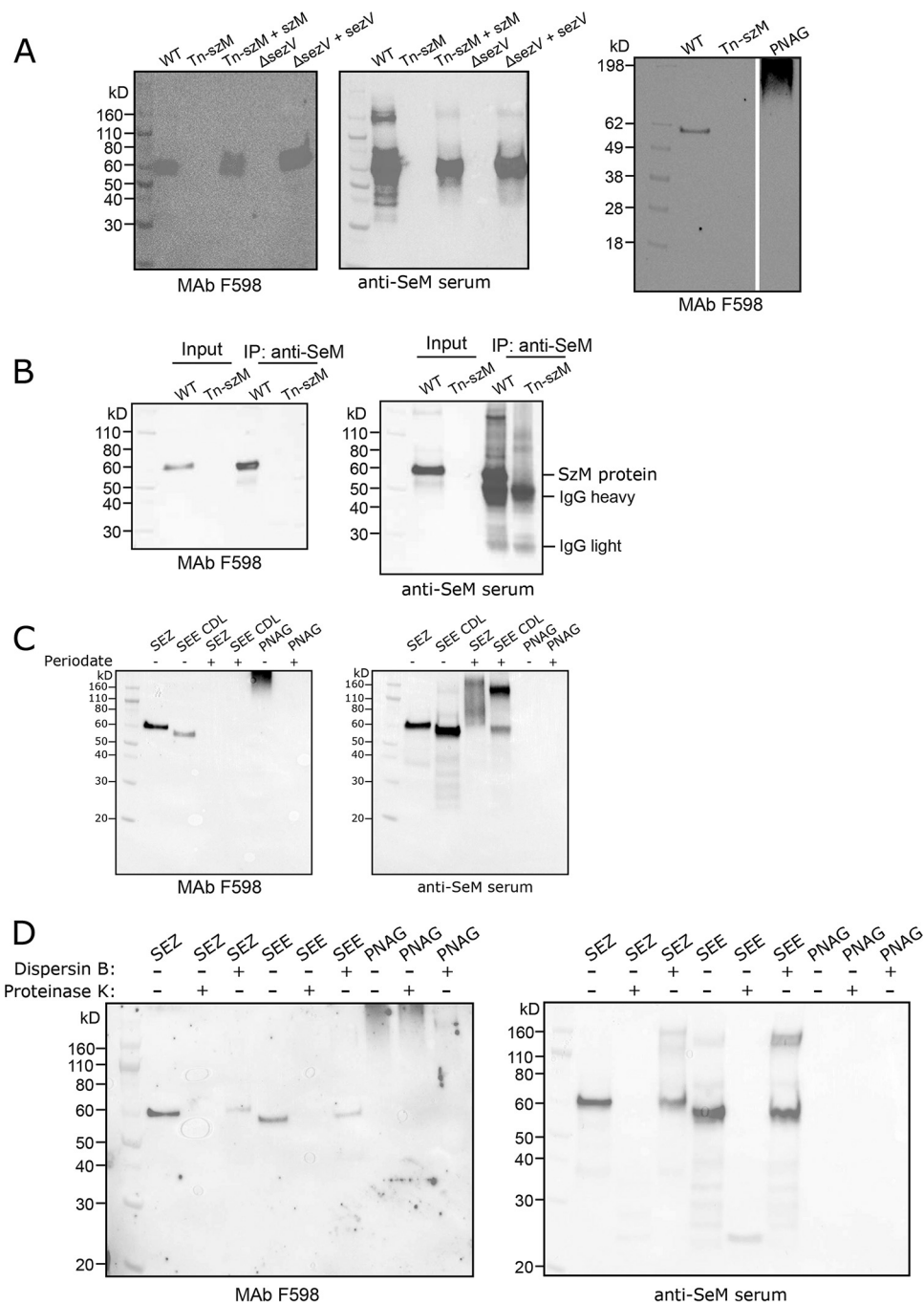


**FIG 4** SzM is directly bound by an anti-PNAG antibody. (A) Western blot of bacterial lysates from SEZ strains. Electrophoresed lysates from the indicated strains were run in duplicate on a single SDS-PAGE gel, transferred to a single membrane, which was cut into two parts; each half was blotted with the indicated antibody. (B) Western blot of immunoprecipitated SzM from SEZ WT and Tn-szM strains after SDS-Page. (C) Western blot of bacterial lysates of SEZ, SEE strain CDL, or purified PNAG carbohydrate with (+) or without (-) periodate treatment. (D) Western blot of bacterial lysates of SEZ, SEE strain CDL, or purified PNAG carbohydrate with (+) or without (-) treatment with either the dispersin B or proteinase K enzymes.

only a minor reduction in binding of the anti-SeM antibody (Fig. 4D). Protease treatment ablated reactivity with both F598 and anti-SeM sera but had minimal effect on purified PNAG polysaccharide. Together, these immunochemical experiments on carbohydrate- and protein-specific degradative enzymes' effects on binding of F598 suggest that SzM and SeM are modified by a carbohydrate with a chemical composition

similar to PNAG. Importantly however, we did not detect either O- or N-linked glycans in mass spectrometry analyses of purified SzM protein (Fig. S3E). Thus, we cannot definitively conclude that these M-like proteins are glycosylated.

**Conservation of and variation in *sezV* and *szM/seM/spa*.** Given the importance of *sezV* and *szM* in SEZ virulence, we investigated whether orthologs of these virulence-linked genes exist in publicly available streptococcal genomes. Notably, homologs of *szM/seM/spa* or *sezV*, based on DNA sequence, were restricted to SEZ and SEE in GCS and a subset of GAS strains. We did not find *szM* or *sezV* homologs in any other streptococcal species or Lancefield groups, or in *Lactococcus* or *Enterococcus*, two related genera (Fig. 5A). All strains with *szM* orthologs harbored an adjacent and divergently oriented *sezV* (Fig. S4A and B), suggesting that *SezV* regulation of SzM is conserved. Among GAS strains, we found that all 15 M18 strains in the database and 1 M36 strain contained the *szM* ortholog (*spa*) and *sezV* (Fig. S4C).

The amino acid sequences of SzM/SeM/Spa and *SezV* from all strains in the database, as well as from 12 newly sequenced strains (see below), were compared. There was considerable variation in the 289 SzM/SeM/Spa amino acid sequences analyzed (Table S2). These M-like sequences could be divided into three classes (Fig. 5B). Most of the sequences ( $n = 274$ ) were similar to SzM from SEZ ATCC 35246; the two other classes, which included seven and eight proteins, respectively, were primarily found in SEZ strains and also encoded adjacent to a *sezV* ortholog. Some strains with truncated SeM/Spa variants were identified (Fig. S4D), which may contribute to the persistence of these strains in their hosts (41), but these were not included in the analyses below.

There were 66 variants found among the 264 full-length class I SzM/SeM/Spa proteins (Fig. S4E and F). No variants were found in common between species (Fig. S4F). Multiple sequence alignment of the amino acid sequences of the SzM/SeM/Spa variants revealed that most of the variation was found in their respective N termini beginning after their signal sequences (SS) (Fig. 5C), concordant with observations regarding SeM proteins in several SEE strains (42, 43). The highest similarity in the SzM/SeM/Spa proteins was found in their signal sequences, coiled-coil domains, and C-terminal cell wall- and cell membrane-spanning regions (W) (Fig. 5C). The coiled-coil domains contain recognizable A and B repeats, regions of short repeated sequences previously identified in SeM/SzM proteins found in SEE and SEZ (9, 16).

In general, the 289 *SezV* proteins analyzed exhibited more conservation than the SzM/SeM/Spa proteins (Fig. S5A and Table S2) and have domain organizations and lengths similar to those of *SezV* from SEZ ATCC 35246. Thus, *sezV* appears to be a conserved transcriptional regulator. However, 39 variants with single amino acid substitutions or small deletions were identified (Fig. S5B), along with several loci that contained more severe changes (Fig. S5C and D).

**SzM/SeM/Spa is recognized by the antibody to PNAG in SEZ, SEE, and M18 GAS strains.** Given the presence of *szM* and *sezV* orthologs in SEZ, SEE, and M18 GAS strains, we investigated whether MAb F598 to PNAG recognized SzM-related proteins from additional strains. Western blots of bacterial lysates derived from eight SEZ and SEE strains isolated from horses with anti-SeM sera detected proteins of ~50 to 60 kDa in all strains but longer exposures were needed to detect the reactive band in some SEZ isolates (e.g., SEZ 14102 and 17006, Fig. 6A; Fig. S6A), whose SzM/SeM amino acid sequences differed more from that of SEZ ATCC 35246 (WT) than those from the other SEE isolates. Notably, F598 recognized a protein of size similar to that of the SzM reactive band in all strains tested except for SEZ 14102, an isolate whose SzM sequence contained a 59-amino-acid deletion (Fig. 6A; Fig. S6B). Thus, the anti-PNAG F598 antibody is broadly reactive with diverse SzM/SeM proteins from equine SEZ and SEE isolates.

We also investigated the expression of M and Spa proteins in M18 GAS isolates and whether MAb F598 bound to any of these proteins. The genomes of five clinical M18 isolates were sequenced and assembled (Fig. S7A). All five of these M18 strains contained linked and divergently oriented *sezV* and *szM* orthologs (*spa*). The locus

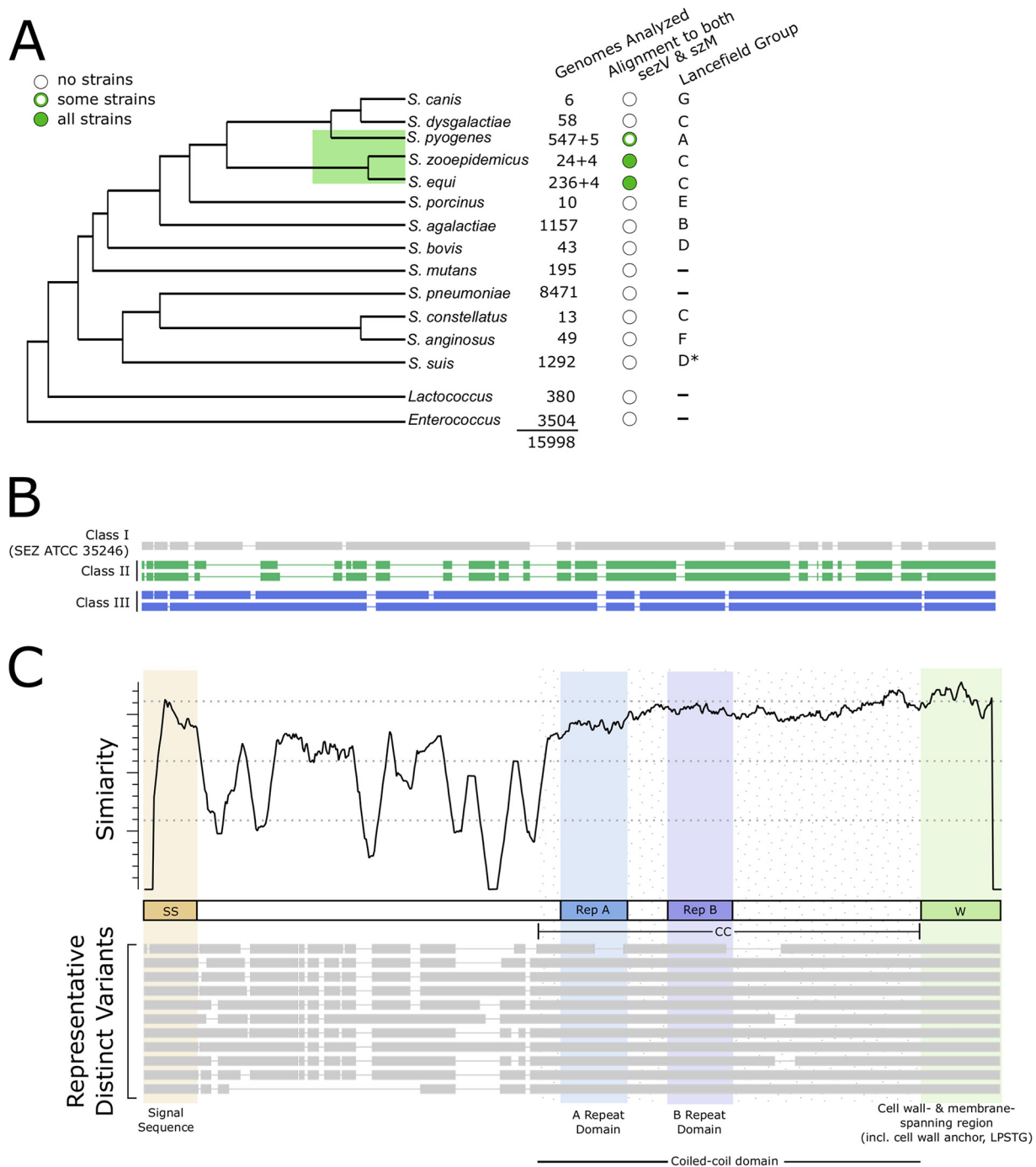


**FIG 5** Conservation of *szM/seM/spa* and *sezV*. (A) Conservation of *sezV* and *szM/seM/spa* across various streptococcal species and Lancefield groups and closely related genera. The cladogram is for illustrative purposes and shows a qualitative representation of the relatedness of the species and genera; it was constructed based on the reports of Gao et al. (70) and Hug et al. (71). Branch lengths are not drawn to scale, nor are they a representation of the true genetic distances between species and strains. The genomes analyzed indicate the numbers of genomes queried in each species; +X represents the number of strains newly sequenced in this study. An alignment to *sezV* and *szM* indicates species that have similarity to both genes. Lancefield groups are as reported by Facklam (72) and Okura et al. (73). \*, *S. suis* was formerly classified as group D (73). (B) Three classes of SzM/SeM/Spa-related proteins encoded adjacent to *sezV*. Visualization of multiple sequence alignment between representative members of each of the three protein clusters demonstrates large differences between clusters and similarity within clusters. Lines represent gaps in the multiple sequence alignment; blocks represent continuous sequences. (C) Amino acid sequence variation in SzM/SeM/Spa proteins. (Top) Similarity plot of amino acids at each position in the protein across all variants of the protein. Similarity (y axis) represents the relative sequence conservation over a set of adjacent residues; a higher value indicates more conservation. (Middle) Schematic of SzM/SeM/Spa with labeled and shaded domains and regions. SS, signal sequence, which contains YSIRK motif; Rep A/B, repeat A/B; CC, predicted coiled-coil domain; W, cell wall- and cell membrane-spanning region, which contains LPXTG motif. Delineations of regions are based on previously published reports (16, 43, 74); the coiled-coil domain was determined by MARCOIL (75). (Bottom) A multiple sequence alignment of representative SzM/SeM/Spa variants demonstrates various domain/region architectures present across the variants. The lines represent gaps in the multiple sequence alignment; the blocks represent continuous sequences.

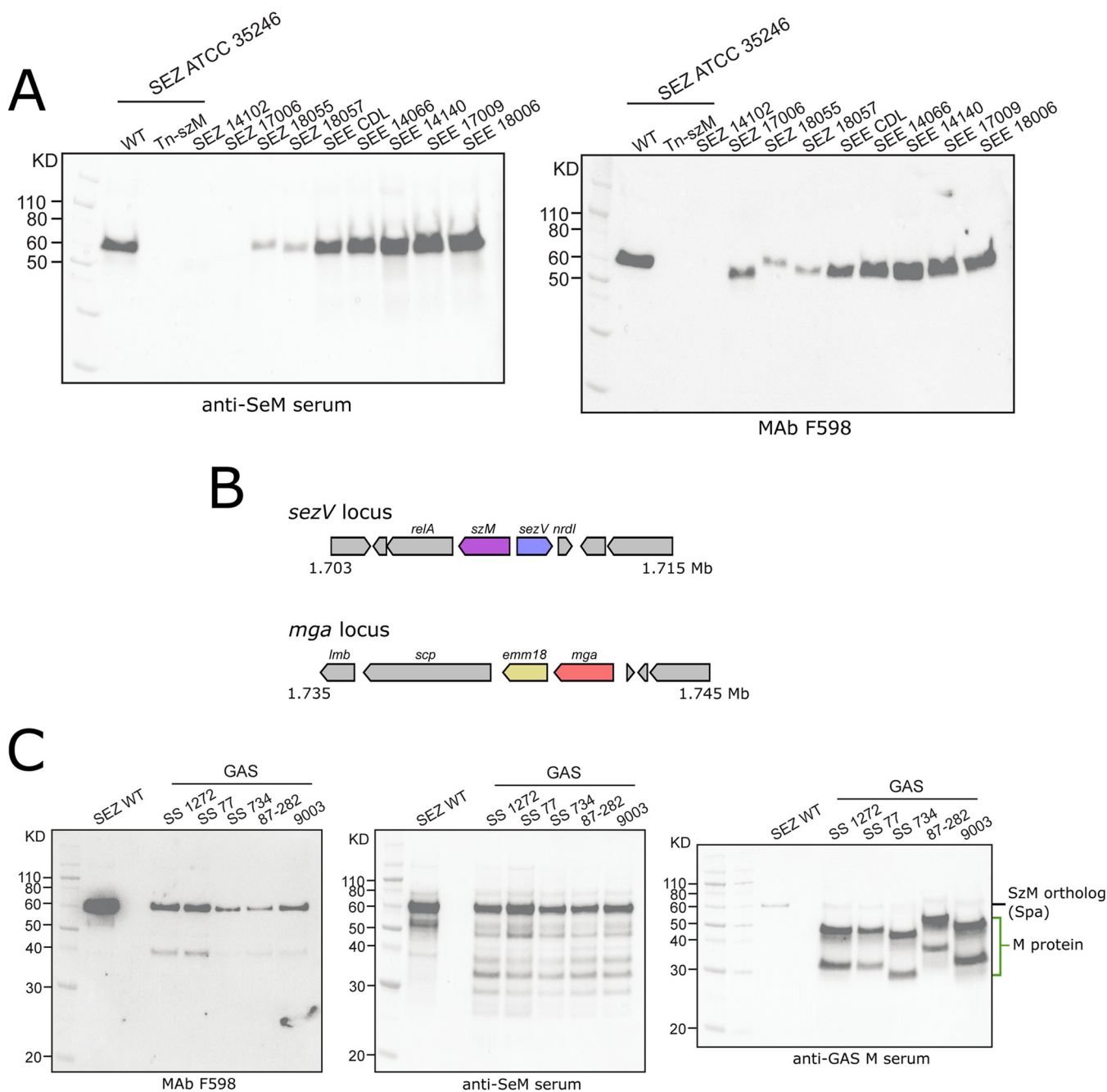


**FIG 6** Anti-PNAG antibody binds SzM/SeM/Spa in several SEZ, SEE, and GAS strains. (A) Western blots of bacterial lysates of the indicated SEZ and SEE strains after SDS-PAGE with anti-SeM or F598 antibodies. (B) Genomic context of the *sezV*, *spa* (the *szM* ortholog), and *mga* loci in a canonical M18 GAS strain, MGAS8232 (76). (C) Western blots of bacterial lysates of the indicated SEZ and newly sequenced M18 GAS strains with F598, anti-SeM, or anti-GAS M antibodies. The anti-GAS M serum was sera raised against a purified, canonical GAS M protein. Lower bands in GAS strains may be indicative of M protein degradation products, as seen previously (18).

containing *sezV* and *spa* was not linked to the locus encoding the canonical M18 M protein (*emm*) or its associated regulator, *mga* (Fig. 6B). Western blotting of lysates from these five strains with the F598 MAb revealed an ~60-kDa band, whereas blots with the isotype control MAb F429 were negative (Fig. 6C; Fig. S7B). A very similar-sized band was also detected in blots using anti-SeM serum; this serum also weakly reacted with bands of ~46 and 34 kDa, which likely correspond to the M18 protein because bands of these sizes were seen in blots with anti-M18 antisera (Fig. 6C). Notably, however, these two bands (likely corresponding to the M18 protein) were not detected with the

anti-PNAG antibody. Thus, these M18 GAS strains appear to express at least two M-like proteins, the canonical M18 M protein, which is not recognized by F598, and Spa, which is bound by this anti-PNAG MAb.

## DISCUSSION

Our investigation of genes required for surface PNAG reactivity in a porcine SEZ isolate led to the identification of *szM*, which encodes an M-like protein and its linked activator *sezV*. SzM/SeM/Spa (also called FgBP) is representative of a class of M-like proteins distinct from M, Mrp, and Enn. SzM/SeM/Spa proteins appear to be decorated with a PNAG-like oligosaccharide, although this conclusion is based on immunochemical analysis rather than definitive chemical isolation of an oligosaccharide associated with these M-like proteins. Both *szM* and *sezV* are required for robust SEZ virulence, and homologues of these linked virulence genes were identified in all SEZ, SEE, and M18 GAS genomes in the database. Thus, the *szM/seM/spa* and *sezV* loci appear to define a subtype of virulent streptococci.

We used labeled MAb F598 to PNAG to carry out a FACS-based screen of a Tn library in SEZ strain ATCC 35426 to identify insertion mutants that were deficient in surface expression of PNAG. The screen appeared to work well, and even after one round of selection, mutants lacking F598 binding were identified (Fig. 1C); after three rounds of selection, the population was nearly uniformly PNAG negative. However, the library diversity was compromised by Tn jackpots. Linkage between the phenotype (the absence of F598 binding to the Tn insertion mutant) and the genotype (the site of transposon insertion) was not established for several insertions. Whole-genome sequencing led to the identification of mutations in the *sezV* and *szM* loci that were shared among independently derived PNAG-negative SEZ mutants. We were unable to enrich for PNAG-negative cells when a WT (nonmutagenized) SEZ culture was FACS sorted, and it is not clear why PNAG-negative mutants were easily detected in the Tn library.

Although *SezV* lacks sequence similarity to *Mga*, it appears to be a functional analogue of this central GAS virulence activator. In GAS, *Mga* activates expression of virulence-associated and linked M and M-like proteins (*Mrp* and *Enn*) (44, 45). Like *Mga*, *SezV* proved to be a critical activator of *SzM* expression and to be required for SEZ virulence in mice. The *SezV* regulon was relatively small since *szM* was the only locus with a >5-fold reduction in transcript levels in the absence of *sezV*. *SezV* does not appear to regulate expression of *SzP*, the other M-like protein in SEZ/SEE, suggesting that there are additional SEZ virulence regulators that have yet to be identified. *SezV* also appears to downregulate (directly or indirectly) the expression of several genes, including an operon coding for the synthesis of a *cne*-containing fimbrial *Fim1* pilus. It is tempting to speculate that the *SezV* coordinated induction of *SzM* expression and repression of pilus expression corresponds to a SEZ virulence program that facilitates the organism's dissemination from sites, such as the oropharynx, where it is a commensal, to sites such as the bloodstream, lungs, and brain, where it is pathogenic. The presence of the predicted sensor kinase-like domain in *SezV* suggests the possibility that there may be host-derived stimuli that trigger *SezV* activity.

The key role of *SzM* in SEZ virulence was not known, but a *SzM* homologue in SEE (*SeM*) has been linked to virulence (16, 17). In addition, McLellan et al. (19) found that *Spa*, a *SzM* homolog in M18 GAS, appears to play a more substantial role in pathogenicity than the canonical M18 protein. Similar to canonical M proteins, *SzM* proteins likely promote virulence through their immunomodulatory functions. Timoney and coworkers have demonstrated that *SzM* from SEZ strain NC78 can inhibit phagocytosis and bind to and modify the activity of components of the coagulation cascade such as plasminogen (9, 14). In addition to roles in pathogenicity, *SzM/SeM/Spa* proteins from SEZ, SEE, and M18 GAS strains have proven to be effective immunogens eliciting protective immune responses (9, 14, 16, 18). Our analysis of *SzM/SeM/Spa* sequences from ~300 strains revealed that the highest variability is present in the N-terminal regions, whereas the C-terminal coiled-coil domains are more conserved.

There appears to be greater variability in SEZ versus SEE, which is consistent with the idea that SEZ as a whole is more genetically variable than SEE (Fig. S4E).

Unexpectedly, SzM and its activator SezV answered the screen for mutants that were not bound by an MAb (F598) to PNAG. Two observations lend support to the idea that SzM is decorated by a PNAG-like carbohydrate. First, purified SzM was bound by F598, whereas F429, an isotype-matched control antibody that includes identical constant regions as F598 bound with much lower affinity. Second, periodate and dispersin B, reagents that cleave carbohydrates, ablated SzM's reactivity with MAb F598 but not to anti-SeM sera. Specific glycosylation of proteins with oligomers of PNAG (or a related oligosaccharide) has not been described, but O-glycosylation of a streptococcal adhesin has been reported (46). However, it is premature to conclude that SzM is decorated by a PNAG-related oligosaccharide. We did not identify N- or O-linked oligosaccharides bound to SzM by mass spectrometry, and the transposon screen did not yield genes obviously implicated in the synthesis of a polysaccharide. Regardless of whether F598 is recognizing an oligosaccharide linked to SzM, our observation that this antibody binds to a wide range of SEZ, SEE, and M18 GAS strains raises the possibility that immunity to PNAG may have therapeutic applications in animal and human diseases caused by streptococci bearing SzM-like M proteins.

## MATERIALS AND METHODS

**Bacterial strains and growth.** Bacterial strains are listed in Table S3 in the supplemental material. Streptococcal bacteria were routinely grown aerobically in THY (Todd-Hewitt broth plus 0.5% yeast extract) media with shaking or THY agar at 37°C. For GAS strains, liquid cultures were grown aerobically without agitation at 37°C. Antibiotics, when used, were included at the following concentrations: spectinomycin (Spc), 100 µg/ml; or kanamycin (Km), 300 µg/ml. *E. coli* bacteria were routinely grown in lysogeny broth (LB) media or agar. Antibiotics were used at the following concentrations: carbenicillin (Carb), 100 µg/ml; or Km, 50 µg/ml.

For growth curves, a fresh colony was picked, inoculated in THY media, and grown to log-phase (4 to 6 h) at 37°C. After harvesting by centrifugation, the supernatant was discarded, and each pellet was resuspended in fresh THY to an optical density at 600 nm (OD<sub>600</sub>) of 0.50 and then diluted 10× with the same medium to an OD<sub>600</sub> of ~0.05. Then, 200 µl of culture was added per well of a honeycomb plate, with five replicates for each sample. A Bioscreen C (Growth Curves USA) growth curve machine was used to measure the OD<sub>600</sub> over 24 h, with measurements every 10 min.

**Immunofluorescence microscopy.** Stationary-phase bacteria were labeled with F598 or F429 conjugated to AF488 at room temperature for 4 h after being fixed in ice-cold methanol for 1 min. Widefield microscopy was performed on a Nikon Eclipse Ti microscope. Slides were fixed in ProLong Diamond antifade mountant with DAPI (4',6'-diamidino-2-phenylindole; Invitrogen).

**Transposon library construction.** A transposon library was constructed in SEZ ATCC 35246 using pMar4s transposon plasmids by modifying a method used for Tn library construction in GAS (30, 47). A detailed graphical depiction of the method can be found in Fig. S1A. Briefly, 1 µg of purified pMar4s plasmid was electroporated into SEZ. Transformants were resuspended in 5 ml of THY plus 10% sucrose recovery broth and then cultured at 28°C for 4 h. Bacteria were spread on a THY plate with Km and Spc after dilution, followed by incubation at 28°C for 3 days. More than 100 individual colonies were screened to verify that pMar4s was present as an independent plasmid (i.e., it had not yet undergone integration or transposition). Each colony was streaked onto six different plates with various antibiotics and grown at 28°C for 3 days or overnight at 37°C, as shown in Fig. S1A. Colonies that were unable to grow on a THY+Spc plate at 37°C were collected from Spc and Km THY plates, and frozen stocks were made (25% glycerol). After re-verifying the antibiotic resistance profile of the frozen stock strains, a final Tn library was constructed by spreading  $>5.4 \times 10^5$  colonies from a frozen stock onto 245-cm<sup>2</sup> square plates (Corning) of THY media, followed by incubation at 37°C overnight. Colonies were scraped from the plate with THY broth and mixed; then, after the addition of glycerol (25% final concentration), the library was frozen at -80°C.

**FACS-based PNAG screen.** Flow cytometry and FACS were performed on a Sony SH800S cell sorter. For routine measurement of antibody binding, live bacteria were labeled with MAb F598 or F429 conjugated to Alexa Fluor 488 (AF488). FACS enrichment of the SEZ transposon library was conducted as follows. An aliquot of the library was stained with AF488-F598 prior to loading on the FACS. From bacteria whose fluorescence intensity was below a specified threshold, the lowest ~10% (screen A) and ~20% (screen B) of AF488-F598 labeled bacteria were collected. After enrichment, the bacteria were outgrown overnight either in liquid THY plus 1% dextrose media (A) or on solid THY plates (B) prior to re-enrichment by FACS using a threshold similar to that used for the first round. For bacteria grown on solid THY, prior to FACS sorting, the bacteria were scraped from the plate and resuspended in THY media. With each round, the percentage of bacteria that were below the threshold increased. There were two rounds of selection for screen A and three rounds for screen B. Bacteria from each round and the input were collected, and genomic DNA was extracted for Tn-seq. Several individual bacterial colonies from the final round of each screen were also picked and stored as frozen stocks. Some of these non-F598-binding

strains were subjected to WGS, leading to bacterial strains with transposon insertions in RS01795, *sezV* (RS09465), and *szM* (RS09460).

**Tn-seq analysis.** Tn-seq library construction and data analysis was performed as previously described (48–50). Briefly, genomic DNA was extracted, transposon junctions were amplified (a custom primer, Himmer3outMar, was designed for the pMar4s transposon plasmid), sequencing was performed on an Illumina MiSeq, and data were analyzed using a modified ARTIST pipeline. Sequence reads were mapped onto the SEZ ATCC 35246 genome. Reads at each TA site were tallied and assigned to annotated genes. We sequenced the original Tn library, as well as the input Tn library used for the FACS screen (a thawed aliquot of the original Tn library) and the output Tn libraries after FACS selection for absence of F598 binding. For each output sample, a multinomial distribution based on the distribution in the output sample was used to resample reads in the corresponding input sample multiple times and total reads in the simulated inputs was adjusted to match that of the respective output sample. A Mann-Whitney U (MWU) test was used to identify genes that have significantly different insertion profiles and read distributions between the output and simulated input samples. Note that only sites in which there were nonzero reads in either the simulated input and/or output were used, as has been previously described (48). The  $\log_2$ -fold change was also calculated for each gene based on the reads in the output and simulated input library. Genes were filtered based on their containing at least five TA sites with a representative mutant in the input library, a  $\log_2$ -fold change of at least 1, and an MWU *P* value of at least 0.05.

**Whole-genome sequencing.** Genomic DNA was purified from stationary-phase cultures of bacteria using a MasterPure Gram-positive DNA purification kit (Epicentre, catalog no. MGP04100). The DNA concentration was adjusted prior to library preparation and sequencing at the Biopolymers Facility at Harvard Medical School. Libraries were constructed using the Nextera XT kit (Illumina), and paired-end sequencing was performed on a MiSeq (Illumina) with dual-indexing and  $2 \times 75$ -bp reads. Reads were mapped to the SEZ ATCC 35246 reference genome using bwa (51). Nucleotide variants were called as previously described (50), using GATK (v3.5) (52), annotated using ANNOVAR (53), and filtered and compared using vcftools (54). To identify transposon insertions in WGS reads, the reads were processed as for Tn-seq analysis. Putative mutations that result in loss of MAb F598 binding were found by identifying mutations present in the strains that could not bind F598 and absent from strains that could bind F598. For newly sequenced GAS strains, libraries were prepared and sequenced as for SEZ strains. However, in this case, Illumina reads were trimmed with sickle (v1.33) (55) and assembled using SPADES (v3.11.1) (56). Quast (v5.0.2) (57) was used to determine the assembly statistics.

**Strain construction.** Single gene deletions in SEZ ATCC 35246 were constructed as previously described (39) using the temperature-sensitive shuttle plasmid pSET4s (58). Upstream and downstream regions of each gene were cloned into pSET4s, which confers Spc resistance. The constructed plasmids were introduced into competent SEZ cells via electroporation using the following settings: voltage, 2,500 V; capacitance, 25  $\mu$ F; and resistance, 200  $\Omega$ . The transformed bacteria were grown at 37°C in THY broth plus Spc to generate single-crossover mutants. Double-crossover mutants were generated by repeatedly passaging the single-crossover strains at 28°C on THY without Spc. The gene deletions were verified by PCR and Sanger sequencing.

To construct complementation plasmids, the *sezV* and *szM* genes were amplified by PCR from SEZ ATCC 35246 genomic DNA and inserted into the pSET2 plasmid (59). For the *szM* gene, the constructed plasmid was amplified in *E. coli* DH5 $\alpha$  before electroporation into SEZ. For the *sezV* gene, a dialyzed Gibson assembly production of pSET2 and *sezV* was used to directly transform SEZ. For complementation with RS00930, the RS00930 gene, containing a synonymous amino acid mutation, was cloned into pSET4s and used to restore the RS00930 gene in its native chromosomal locus.

PCR was routinely performed using Phusion high-fidelity DNA polymerase (NEB), and plasmids were constructed via Gibson assembly using the NEBuilder HiFi DNA assembly master mix (NEB). Primer sequences are listed in Table S3 in the supplemental material.

**Electron microscopy.** Bacterial samples were submitted to the electron microscopy facility at Harvard Medical School as colonies grown on solid medium THY plates. SEM was performed on bacterial samples fixed via glutaraldehyde.

**Quantitative RT-PCR.** RNA was isolated from 3-ml log-phase cultures of bacteria. After harvesting bacteria via centrifugation, 50 mg of 0.1-mm glass beads were added to the tube, along with 1 ml of TRIzol (Invitrogen). After homogenization of the mixture vigorously for 2 min, chloroform extraction was performed, followed by purification using an RNeasy kit (Qiagen). The RNA was subject to DNase treatment and then reverse transcribed using SuperScript II RT (Invitrogen). Fast SYBR green master mix was used for qPCRs, and all reactions were conducted with an ABI StepOne real-time PCR system. The primers used for qPCR are shown in Table S3.

**RNA sequencing.** RNA was isolated from log-phase cultures of bacteria as described above for qPCR. RNA-seq library construction and sequencing was performed by Genewiz, Inc. Briefly, RNA was depleted of rRNA using an Illumina RiboZero kit, and sequencing libraries were prepared using an NEBNext Ultra kit. Paired-end sequencing of libraries was performed on a single lane of a HiSeq 4000 (Illumina) with single-indexing and  $2 \times 150$  bp reads. The total reads per sample were  $\sim 40+$  million, which is well above the number recommended for bacterial differential gene analysis given the genome size of SEZ (60). Reads were mapped to the SEZ ATCC 35246 genome using bwa-mem (51), and read counts per gene were generated using the Rsubread package (v1.34.6) (61) in the R computing environment. Differential gene analysis was performed using the DESeq2 package (v1.24.0) (62) in R. Genes were filtered based on outputs of DESeq2, using a  $\log_2$ -fold change magnitude of 1 and an adjusted *P* value of 0.05. A volcano plot was generated using the EnhancedVolcano package in R.

**Animal experiments.** Female C57BL/6J mice (6 to 8 weeks old) obtained from the Jackson Laboratory were used for all experiments. Animal experiments were performed as previously described (39), using protocols approved by the BWH IACUC. Mouse experiments were conducted according to the recommendations of the National Institutes of Health *Guide for the Care and Use of Laboratory Animals*. Adult mice were euthanized via isoflurane inhalation and subsequent cervical dislocation. i.v. infections were performed via tail-vein injection of  $10^7$  CFU of log-phase bacteria. To determine tissue burdens, the animals were sacrificed at 24 h after inoculation and dissected, the tissues were homogenized, and serial dilutions of the homogenates were plated on THY media to enumerate bacterial CFU. For the bacterial burden in the blood, prior to sacking, 20  $\mu$ l of blood was drawn and serial dilutions were plated on THY media.

Data from animal experiments was analyzed in Prism (v8; GraphPad). The Mantel-Cox was used for statistical analyses of the Kaplan-Meier survival curves, and a Kruskal-Wallis test with Dunn's multiple-comparison test was used to compare tissue CFU burdens.

**Western blots.** LDS loading dye (NEB) was added to samples, which were then boiled at 95°C for 10 min prior to running on SDS-PAGE gels. Either Novex Sharp prestained protein standard (Invitrogen) or SeeBlue prestained protein standard (Invitrogen) were used as molecular weight markers. Transfer was performed using the iBlot2 (Thermo Fisher Scientific) system. Membranes were blocked in 1% bovine serum albumin plus 5% powdered milk prior to blotting with primary antibodies. Antibodies were used at the following concentrations: F598 (13  $\mu$ g/ml), F429 (13  $\mu$ g/ml), anti-SeM sera (1:1,000), anti-M sera (1:1,000), horseradish peroxidase (HRP)-conjugated goat anti-rabbit IgG antibody (1:10,000, ab6858; Abcam), and HRP-conjugated goat anti-human IgG antibody (1:10,000, A4914; Sigma). The anti-SeM and anti-M sera were both gifts from Gunnar Lindahl. The anti-SeM serum was raised against the full-length SeM protein. The anti-M serum (13) was raised against the C-terminal BCW region, which contains B repeats, the conserved C repeat, and the conserved W (wall-spanning) region of the *S. pyogenes* M5 protein. SuperSignal chemiluminescent substrates (Thermo Fisher Scientific) were used as the HRP substrates. Gels and Western blots were imaged using the ChemiDoc imaging system (Bio-Rad).

**Immunoprecipitation.** A portion (50 ml) of overnight-cultured bacteria was harvested by centrifugation at  $16,000 \times g$  for 2 min. After discarding the supernatant and resuspending the pellet in 1 ml of 0.5 M EDTA, the samples were boiled for 5 min to lyse the cells and then centrifuged at  $\sim 20,000 \times g$  for 5 min, and the resulting supernatants were used as the bacterial lysates. The lysates were filtered through an Amicon Ultra-4 10K centrifugal filter device to remove EDTA and then mixed with PBS-T (phosphate-buffered saline [pH 7.4] with 0.01% Tween 20). Dynabeads-protein G (Invitrogen) were used for immunoprecipitation. Briefly, 5  $\mu$ g of F598 or 5  $\mu$ l of anti-M serum were diluted in 200  $\mu$ l of PBS-T and rotated for 30 min with 50  $\mu$ l of magnetic beads at room temperature. The beads were washed once with 200  $\mu$ l of PBS-T. After removing the supernatant with a magnet rack and adding 1 ml of bacterial lysate with protease inhibitors, the mixture was incubated with rotation for 1 h at room temperature or overnight at 4°C to allow the antigen to bind to the magnetic bead-Ab complex. The beads were washed three times with PBS-T and then eluted by adding 20  $\mu$ l of 50 mM glycine (pH 2.8), followed by incubation at 70°C for 10 min.

**Periodate and dispersin B treatments.** Bacterial lysates or purified PNAG polysaccharide were mixed with 0.4 M periodate dissolved in PBS at 1:1 (vol/vol), followed by incubation at 37°C for 1 h. The final concentration of dispersin B used for bacterial lysate or PNAG polysaccharide treatment was 500  $\mu$ g/ml, and samples were incubated at 37°C for 24 h.

**Computational analyses.** The nucleotide sequence of the *sezV-szM* locus from ATCC 35246 plus an additional flanking sequence was used as a query in blastn searches of the NCBI complete and WGS prokaryotic genomes to identify strains of streptococci and related genera that contain the two *szM/seM/spa* and *sezV* genes. Thresholds for identifying homologs were an alignment of >200 nucleotides for *szM* and an alignment of >300 nucleotides for *sezV*. These settings yielded only one homolog in each strain that contained a homolog. *SzM* homologs were not identified in some strains using more stringent settings; these strains were subsequently identified as containing class II or III *szM* homologs. Protein sequences were aligned using MUSCLE (v3.8.31) (63). Sequence alignments were visualized in Seaview (v4.7) (64) and Genome Workbench (v3.0.0; NCBI).

Protein sequences were clustered with MMSeqs2 (65, 66) using the normal/slow sensitive settings. For identification of representative alleles, 80% minimum sequence identity and 80% minimum alignment coverage was used. For identification of distinct classes of *szM/seM/spa*, the thresholds were both adjusted to 50%. The similarity of amino acids across a multiple sequence alignment was assessed using plotcon (67). Similarity (*y* axis) represents the sequence conservation over a set of adjacent residues. The similarity at one position is calculated as the average of all possible pairwise substitution scores (taken from a similarity matrix) of the residues at the position. The average of position similarities over a set of adjacent residues is graphed in Fig. 5C and Fig. 5SA.

Distance between the *szM/seM/spa* and *sezV* genes was determined as the distance between the first base of either gene that occurred first in the strain's genome and the first base of the second gene. Orientation of transcription of the *szM/seM/spa* and *sezV* genes was determined based on genomic annotations and subsequently compared, taking into account the order in which the genes occurred in the genome.

Identification of the loci in newly sequenced and assembled streptococcal strains was performed using blastn from blast+ (v2.7.1; NCBI). Open reading frames were identified using ORFfinder (NCBI). *emm* (M protein) typing was performed by identifying the annotated M protein in the strain and the CDC *emm* blast server (Streptococcus Group A Subtyping Request Form BLAST 2.0 Server; <https://www2a.cdc.gov/ncidod/biotech/strepblast.asp>). For newly sequenced GAS strains, the M protein was identified



using blast+ (tblastn), the top hit was chosen, and the sequence was then input into the CDC *emm* blast server to type the strain.

M18 strains were identified among the GAS strains using tblastn. The M protein from MGAS 8232 was used as the query sequence to identify additional M18 strains. Thresholds for the E value and the percent identity were lowered until the aligned M protein sequence began to be mapped to a different *emm* type, which was determined manually by inputting the M protein sequences into the CDC *emm* blast server. Based on the final thresholds, a total of 15 M18 strains were identified among the GAS strains analyzed.

**Mass spectrometry.** Mass spectrometry of immunoprecipitated and gel-purified SzM was carried out at the Taplin Biological Mass Spectrometry Facility, Harvard Medical School. In-gel trypsin digestion was performed prior to mass spectrometry analysis. Analysis of O-linked and N-linked glycans on SzM was performed at the National Center for Functional Glycomics. Briefly, N- and O-linked glycans were obtained from SzM and fetuin, a control glycosylated protein, by treating proteins with PNGase F to obtain the N-link glycans and then subsequently with sodium borohydride (NaBH<sub>4</sub>) to obtain the O-linked glycans.

**Data availability.** Illumina reads for the WGS and RNA-seq experiments have been uploaded to the NCBI Short Read Archive (SRA) under BioSample accession numbers SAMN12770224-25, SAMN12772038-42, and SAMN12784884-89.

## SUPPLEMENTAL MATERIAL

Supplemental material for this article may be found at <https://doi.org/10.1128/mBio.02500-19>.

**FIG S1**, EPS file, 0.3 MB.

**FIG S2**, EPS file, 0.4 MB.

**FIG S3**, EPS file, 1.4 MB.

**FIG S4**, EPS file, 0.2 MB.

**FIG S5**, EPS file, 0.1 MB.

**FIG S6**, EPS file, 1.5 MB.

**FIG S7**, EPS file, 0.7 MB.

**TABLE S1**, XLSX file, 0.5 MB.

**TABLE S2**, XLSX file, 0.04 MB.

**TABLE S3**, XLSX file, 0.01 MB.

## ACKNOWLEDGMENTS

This study was supported by the National Natural Science Foundation of China (31772746 and 31302093), the National Key Research and Development Program (2016YFD0501607 and 2018YFD0500506), the Young Backbone Teachers Study Abroad Program of China Scholarship Council (201706855039), Priority Academic Program Development of Jiangsu Higher Education Institutions (Z.M.), National Institute of General Medical Sciences grant T32GM007753 (J.D.D.), the National Natural Science Foundation of China (31272581), the National Key Research and Development Program (2017YFD0500203; H.F.), and National Institute of Allergy and Infectious Diseases grant R01-AI-043247 and the Howard Hughes Medical Institute (M.K.W.).

We gratefully acknowledge Gunnar Lindahl for providing the anti-SeM sera and anti-M sera, and we thank Michael Wessels for providing the GAS M18 strains (87-282, 9003, SS-77, SS-734, and SS-1272). We thank Gunnar Lindahl and Brigid Davis for insightful comments on the manuscript. We also thank the Harvard Medical School Biopolymers Facility for assistance with whole-genome sequencing, Maria Ericsson and the Harvard Medical School Electron Microscopy Facility for assistance with electron microscopy sample preparation and imaging, the Taplin Biological Mass Spectrometry Facility for mass spectrometry, and the National Center for Research Resources (a part of the National Institutes of Health) for the support of the National Center for Functional Glycomics at Beth Israel Deaconess Medical Center (P41GM103694) which assisted with glycan mass spectrometry.

## REFERENCES

1. Fulde M, Valentin-Weigand P. 2013. Epidemiology and pathogenicity of zoonotic streptococci. *Curr Top Microbiol Immunol* 368:49–81. [https://doi.org/10.1007/82\\_2012\\_277](https://doi.org/10.1007/82_2012_277).
2. Lindahl S, Aspán A, Bäverud V, Ljung H, Paillet R, Pringle J, Söderlund R, Wright NL, Waller AS. 2012. A clonal outbreak of upper respiratory disease in horses caused by *Streptococcus equi* subsp. *zooepidemicus*. *J Equine Vet Sci* 32:S24. <https://doi.org/10.1016/j.jevs.2012.08.057>.
3. Feng ZGH. 1977. Outbreak of swine streptococcosis in Sichan province and identification of pathogen. *Anim Husb Vet Med Lett* 2:7–12.

4. Liu PH, Shun SF, Wang YK, Zhang SH. 2001. Identification of swine *Streptococcus* isolates in Shanghai. *Chin J Vet Med* 21:42–46.
5. Boyle AG, Timoney JF, Newton JR, Hines MT, Waller AS, Buchanan BR. 2018. *Streptococcus equi* infections in horses: guidelines for treatment, control, and prevention of strangles, revised consensus statement. *J Vet Intern Med* 32:633–647. <https://doi.org/10.1111/jvim.15043>.
6. Mori N, Guevara JM, Tilley DH, Briceno JA, Zunt JR, Montano SM. 2013. *Streptococcus equi* subsp. *zooepidemicus* meningitis in Peru. *J Med Microbiol* 62:335–337. <https://doi.org/10.1099/jmm.0.050245-0>.
7. Eyre DW, Kenkre JS, Bowler I, McBride SJ. 2010. *Streptococcus equi* subspecies *zooepidemicus* meningitis: a case report and review of the literature. *Eur J Clin Microbiol Infect Dis* 29:1459–1463. <https://doi.org/10.1007/s10096-010-1037-5>.
8. Boschwitz JS, Timoney JF. 1994. Characterization of the antiphagocytic activity of equine fibrinogen for *Streptococcus equi* subsp. *equi*. *Microb Pathog* 17:121–129. <https://doi.org/10.1006/mpat.1994.1058>.
9. Velineni S, Timoney JF. 2013. Characterization and protective immunogenicity of the Szm protein of *Streptococcus zoepidemicus* NC78 from a clonal outbreak of equine respiratory disease. *Clin Vaccine Immunol* 20:1181–1188. <https://doi.org/10.1128/CI.00069-13>.
10. Timoney JF, Artiushin SC, Boschwitz JS. 1997. Comparison of the sequences and functions of *Streptococcus equi* M-like proteins SeM and SzPse. *Infect Immun* 65:3600–3605.
11. Frost HR, Sanderson-Smith M, Walker M, Botteaux A, Smeesters PR. 2018. Group A streptococcal M-like proteins: from pathogenesis to vaccine potential. *FEMS Microbiol Rev* 42:193–204. <https://doi.org/10.1093/femsre/fux057>.
12. Fischetti VA. 1989. Streptococcal M protein: molecular design and biological behavior. *Clin Microbiol Rev* 2:285–314. <https://doi.org/10.1128/cmr.2.3.285>.
13. Lannergård J, Gustafsson MCU, Waldemarsson J, Norrby-Teglund A, Stålhammar-Carlemalm M, Lindahl G. 2011. The hypervariable region of *Streptococcus pyogenes* M protein escapes antibody attack by antigenic variation and weak immunogenicity. *Cell Host Microbe* 10:147–157. <https://doi.org/10.1016/j.chom.2011.06.011>.
14. Velineni S, Timoney JF. 2013. Identification of novel immunoreactive proteins of streptococcus *zoepidemicus* with potential as vaccine components. *Vaccine* 31:4129–4135. <https://doi.org/10.1016/j.vaccine.2013.06.100>.
15. Hong-Jie F, Fu-Yu T, Ying M, Cheng-Ping L. 2009. Virulence and antigenicity of the *szp*-gene deleted *Streptococcus equi* ssp. *zoepidemicus* mutant in mice. *Vaccine* 27:56–61. <https://doi.org/10.1016/j.vaccine.2008.10.037>.
16. Meehan M, Nowlan P, Owen P. 1998. Affinity purification and characterization of a fibrinogen-binding protein complex which protects mice against lethal challenge with *Streptococcus equi* subsp. *equi*. *Microbiology* 144:993–1003. <https://doi.org/10.1099/00221287-144-4-993>.
17. Meehan M, Owen P, Lynagh Y, Woods C. 2001. The fibrinogen-binding protein (FgBP) of *Streptococcus equi* subsp. *equi* additionally binds IgG and contributes to virulence in a mouse model. *Microbiology* 147:3311–3322. <https://doi.org/10.1099/00221287-147-12-3311>.
18. Dale JB, Chiang EY, Liu S, Courtney HS, Hasty DL. 1999. New protective antigen of group A streptococci. *J Clin Invest* 103:1261–1268. <https://doi.org/10.1172/JCI5118>.
19. McLellan DGJ, Chiang EY, Courtney HS, Hasty DL, Wei SC, Hu MC, Walls MA, Bloom JJ, Dale JB. 2001. Spa contributes to the virulence of type 18 group A streptococci. *Infect Immun* 69:2943–2949. <https://doi.org/10.1128/IAI.69.5.2943-2949.2001>.
20. Simpson WJ, Cleary P. 1987. Expression of M type 12 protein by a group A streptococcus exhibits phaselike variation: evidence for coregulation of colony opacity determinants and M protein. *Infect Immun* 55:2448–2455.
21. Simpson WJ, LaPenta D, Chen C, Cleary P. 1990. Coregulation of type 12 M protein and streptococcal C5a peptidase genes in group A streptococci: evidence for a virulence regulon controlled by the *virR* locus. *J Bacteriol* 172:696–700. <https://doi.org/10.1128/jb.172.2.696-700.1990>.
22. Sabharwal H, Michon F, Nelson D, Dong W, Fuchs K, Manjarrez RC, Sarkar A, Uitz C, Viteri-Jackson A, Suarez RSR, Blake M, Zabriskie JB. 2006. Group A streptococcus (GAS) carbohydrate as an immunogen for protection against GAS infection. *J Infect Dis* 193:129–135. <https://doi.org/10.1086/498618>.
23. van Sorge NM, Cole JN, Kuipers K, Henningham A, Aziz RK, Kasirer-Friede A, Lin L, Berends ETM, Davies MR, Dougan G, Zhang F, Dahesh S, Shaw L, Gin J, Cunningham M, Merriman JA, Hütter J, Lepenies B, Rooijackers SHM, Malley R, Walker MJ, Shattil SJ, Schlievert PM, Choudhury B, Nizet V. 2014. The classical Lancefield antigen of group A streptococcus is a virulence determinant with implications for vaccine design. *Cell Host Microbe* 15:729–740. <https://doi.org/10.1016/j.chom.2014.05.009>.
24. Henningham A, Davies MR, Uchiyama S, van Sorge NM, Lund S, Chen KT, Walker MJ, Cole JN, Nizet V. 2018. Virulence role of the GlcNAc side chain of the Lancefield cell wall carbohydrate antigen in non-M1-serotype group A streptococcus. *mBio* 9:e00294-17.
25. Wei Z, Fu Q, Chen Y, Cong P, Xiao S, Mo D, He Z, Liu X. 2012. The capsule of *Streptococcus equi* ssp. *zoepidemicus* is a target for attenuation in vaccine development. *Vaccine* 30:4670–4675. <https://doi.org/10.1016/j.vaccine.2012.04.092>.
26. Stollerman GH, Dale JB. 2008. The importance of the group A streptococcus capsule in the pathogenesis of human infections: a historical perspective. *Clin Infect Dis* 46:1038–1045. <https://doi.org/10.1086/529194>.
27. Cywes-Bentley C, Skurnik D, Zaidi T, Roux D, DeOliveira RB, Garrett WS, Lu X, O'Malley J, Kinzel K, Zaidi T, Rey A, Perrin C, Fichorova RN, Kayatani AKK, Maira-Litran T, Gening ML, Tsvetkov YE, Nifantiev NE, Bakaletz LO, Pelton SI, Golenbock DT, Pier GB. 2013. Antibody to a conserved antigenic target is protective against diverse prokaryotic and eukaryotic pathogens. *Proc Natl Acad Sci* 110:E2209–E2218. <https://doi.org/10.1073/pnas.1303573110>.
28. Lu X, Skurnik D, Pozzi C, Roux D, Cywes-Bentley C, Ritchie JM, Munera D, Gening ML, Tsvetkov YE, Nifantiev NE, Waldor MK, Pier GB. 2014. A poly-N-acetylglucosamine-Shiga toxin broad-spectrum conjugate vaccine for Shiga toxin-producing *Escherichia coli*. *mBio* 5:1–9. <https://doi.org/10.1128/mBio.00974-14>.
29. Pier GB, Boyer D, Preston M, Coleman FT, Llosa N, Mueschenborn-Koglin S, Theilacker C, Goldenberg H, Uchin J, Priebe GP, Grout M, Posner M, Cavacini L. 2004. Human monoclonal antibodies to *Pseudomonas aeruginosa* alginate that protect against infection by both mucoid and nonmucoid strains. *J Immunol* 173:5671–5678. <https://doi.org/10.4049/jimmunol.173.9.5671>.
30. Liu R, Zhang P, Su Y, Lin H, Zhang H, Yu L, Ma Z, Fan H. 2016. A novel suicide shuttle plasmid for *Streptococcus suis* serotype 2 and *Streptococcus equi* ssp. *zoepidemicus* gene mutation. *Sci Rep* 6:1–9. <https://doi.org/10.1038/srep27133>.
31. Xu B, Pei X, Su Y, Ma Z, Fan H. 2016. Capsule of *Streptococcus equi* subsp. *zoepidemicus* hampers the adherence and invasion of epithelial and endothelial cells and is attenuated during internalization. *FEMS Microbiol Lett* 363:fnw164. <https://doi.org/10.1093/femsle/fnw164>.
32. Swanson J, Hsu KC, Gotschlich EC. 1969. Electron microscopic studies on streptococci. I. M antigen. *J Exp Med* 130:1063–1091. <https://doi.org/10.1084/jem.130.5.1063>.
33. Phillips GN, Flicker PF, Cohen C, Manjula BN, Fischetti VA. 1981. Streptococcal M protein: alpha-helical coiled-coil structure and arrangement on the cell surface. *Proc Natl Acad Sci U S A* 78:4689–4693. <https://doi.org/10.1073/pnas.78.8.4689>.
34. Lannergård J, Frykberg L, Guss B. 2003. CNE, a collagen-binding protein of *Streptococcus equi*. *FEMS Microbiol Lett* 222:69–74. [https://doi.org/10.1016/S0378-1097\(03\)00222-2](https://doi.org/10.1016/S0378-1097(03)00222-2).
35. Steward KF, Robinson C, Maskell DJ, Nenci C, Waller AS. 2017. Investigation of the Fim1 putative pilus locus of *Streptococcus equi* subspecies *equi*. *Microbiology* 163:1217–1228. <https://doi.org/10.1099/mic.0.000506>.
36. Flock M, Karlström A, Lannergård J, Guss B, Flock J-I. 2006. Protective effect of vaccination with recombinant proteins from *Streptococcus equi* subspecies *equi* in a strangles model in the mouse. *Vaccine* 24:4144–4151. <https://doi.org/10.1016/j.vaccine.2006.02.016>.
37. Timoney JF, Qin A, Muthupalani S, Artiushin S. 2007. Vaccine potential of novel surface exposed and secreted proteins of *Streptococcus equi*. *Vaccine* 25:5583–5590. <https://doi.org/10.1016/j.vaccine.2007.02.040>.
38. Guss B, Flock M, Frykberg L, Waller AS, Robinson C, Smith KC, Flock J-I. 2009. Getting to grips with strangles: an effective multi-component recombinant vaccine for the protection of horses from *Streptococcus equi* infection. *PLoS Pathog* 5:e1000584. <https://doi.org/10.1371/journal.ppat.1000584>.
39. Ma Z, Peng J, Yu D, Park JS, Lin H, Xu B, Lu C, Fan H, Waldor MK. 2019. A streptococcal Fic domain-containing protein disrupts blood-brain barrier integrity by activating moesin in endothelial cells. *PLoS Pathog* 15:e1007737. <https://doi.org/10.1371/journal.ppat.1007737>.
40. Ramasubbu N, Thomas LM, Ragnanath C, Kaplan JB. 2005. Structural analysis of dispersin B, a biofilm-releasing glycoside hydrolase from the

- periodontopathogen *Actinobacillus actinomycetemcomitans*. *J Mol Biol* 349:475–486. <https://doi.org/10.1016/j.jmb.2005.03.082>.
41. Harris SR, Parkhill J, Holden MTG, Robinson C, Steward KF, Webb KS, Paillot R, Waller AS. 2015. Genome specialization and decay of the strangles pathogen, *Streptococcus equi*, is driven by persistent infection. *Genome Res* 25:1360–1371. <https://doi.org/10.1101/gr.189803.115>.
  42. Anzai T, Kuwamoto Y, Wada R, Sugita S, Kakuda T, Takai S, Higuchi T, Timoney JF. 2005. Variation in the N-terminal region of an M-like protein of *Streptococcus equi* and evaluation of its potential as a tool in epidemiologic studies. *Am J Vet Res* 66:2167–2171. <https://doi.org/10.2460/ajvr.2005.66.2167>.
  43. Kelly C, Bugg M, Robinson C, Mitchell Z, Davis-Poynter N, Newton JR, Jolley KA, Maiden MCJ, Waller AS. 2006. Sequence variation of the SeM gene of *Streptococcus equi* allows discrimination of the source of strangles outbreaks. *J Clin Microbiol* 44:480–486. <https://doi.org/10.1128/JCM.44.2.480-486.2006>.
  44. Hondorp ER, McIver KS. 2007. The Mga virulence regulon: infection where the grass is greener. *Mol Microbiol* 66:1056–1065. <https://doi.org/10.1111/j.1365-2958.2007.06006.x>.
  45. Hondorp ER, Hou SC, Hause LL, Gera K, Lee CE, McIver KS. 2013. PTS phosphorylation of Mga modulates regulon expression and virulence in the group A streptococcus. *Mol Microbiol* 88:1176–1193. <https://doi.org/10.1111/mmi.12250>.
  46. Zhou M, Wu H. 2009. Glycosylation and biogenesis of a family of serine-rich bacterial adhesins. *Microbiology* 155:317–327. <https://doi.org/10.1099/mic.0.025221-0>.
  47. Le Breton Y, McIver KS. 2013. Genetic manipulation of *Streptococcus pyogenes* (the group A *Streptococcus*, GAS). *Curr Protoc Microbiol* 30:Unit 9D.3.
  48. Hubbard TP, Chao MC, Abel S, Blondel CJ, Abel Zur Wiesch P, Zhou X, Davis BM, Waldor MK. 2016. Genetic analysis of *Vibrio parahaemolyticus* intestinal colonization. *Proc Natl Acad Sci U S A* 113:6283–6288. <https://doi.org/10.1073/pnas.1601718113>.
  49. Kimura S, Waldor MK. 2019. The RNA degradosome promotes tRNA quality control through clearance of hypomodified tRNA. *Proc Natl Acad Sci U S A* 116:1394–1403. <https://doi.org/10.1073/pnas.1814130116>.
  50. Hubbard TP, Billings G, Dörr T, Sit B, Warr AR, Kuehl CJ, Kim M, Delgado F, Mekalanos JJ, Lewnard JA, Waldor MK. 2018. A live vaccine rapidly protects against cholera in an infant rabbit model. *Sci Transl Med* 10:1–11.
  51. Li H, Durbin R. 2009. Fast and accurate short read alignment with Burrows-Wheeler transform. *Bioinformatics* 25:1754–1760. <https://doi.org/10.1093/bioinformatics/btp324>.
  52. DePristo MA, Banks E, Poplin R, Garimella KV, Maguire JR, Hartl C, Philippakis AA, del Angel G, Rivas MA, Hanna M, McKenna A, Fennell TJ, Kernytsky AM, Sivachenko AY, Cibulskis K, Gabriel SB, Altshuler D, Daly MJ. 2011. A framework for variation discovery and genotyping using next-generation DNA sequencing data. *Nat Genet* 43:491–498. <https://doi.org/10.1038/ng.806>.
  53. Wang K, Li M, Hakonarson H. 2010. ANNOVAR: functional annotation of genetic variants from high-throughput sequencing data. *Nucleic Acids Res* 38:e164–e164. <https://doi.org/10.1093/nar/gkq603>.
  54. Danecek P, Auton A, Abecasis G, Albers CA, Banks E, DePristo MA, Handsaker RE, Lunter G, Marth GT, Sherry ST, McVean G, Durbin R. 2011. The variant call format and VCFtools. *Bioinformatics* 27:2156–2158. <https://doi.org/10.1093/bioinformatics/btr330>.
  55. Joshi N, Fass J. 2011. Sickle: a sliding-window, adaptive, quality-based trimming tool for FastQ files.
  56. Nurk S, Bankevich A, Antipov D, Gurevich AA, Korobeynikov A, Lapidus A, Pribelski AD, Pyshkin A, Sirotkin A, Sirotkin Y, Stepanauskas R, Clingenpeel SR, Woyke T, Mclean JS, Lasken R, Tesler G, Alekseyev MA, Pevzner PA. 2013. Assembling single-cell genomes and mini-metagenomes from chimeric MDA products. *J Comput Biol* 20:714–737. <https://doi.org/10.1089/cmb.2013.0084>.
  57. Mikheenko A, Pribelski A, Saveliev V, Antipov D, Gurevich A. 2018. Versatile genome assembly evaluation with QUAST-LG. *Bioinformatics* 34:i142–i150. <https://doi.org/10.1093/bioinformatics/bty266>.
  58. Takamatsu D, Osaki M, Sekizaki T. 2001. Thermosensitive suicide vectors for gene replacement in *Streptococcus suis*. *Plasmid* 46:140–148. <https://doi.org/10.1006/plas.2001.1532>.
  59. Takamatsu D, Osaki M, Sekizaki T. 2001. Construction and characterization of *Streptococcus suis*-*Escherichia coli* shuttle cloning vectors. *Plasmid* 45:101–113. <https://doi.org/10.1006/plas.2000.1510>.
  60. Haas BJ, Chin M, Nusbaum C, Birren BW, Livny J. 2012. How deep is deep enough for RNA-Seq profiling of bacterial transcriptomes? *BMC Genomics* 13:734. <https://doi.org/10.1186/1471-2164-13-734>.
  61. Liao Y, Smyth GK, Shi W. 2019. The R package Rsubread is easier, faster, cheaper, and better for alignment and quantification of RNA sequencing reads. *Nucleic Acids Res* 47:e47–e47. <https://doi.org/10.1093/nar/gkz114>.
  62. Love MI, Huber W, Anders S. 2014. Moderated estimation of fold change and dispersion for RNA-seq data with DESeq2. *Genome Biol* 15:550. <https://doi.org/10.1186/s13059-014-0550-8>.
  63. Edgar RC. 2004. MUSCLE: multiple sequence alignment with high accuracy and high throughput. *Nucleic Acids Res* 32:1792–1797. <https://doi.org/10.1093/nar/gkh340>.
  64. Gouy M, Guindon S, Gascuel O. 2010. SeaView version 4: a multiplatform graphical user interface for sequence alignment and phylogenetic tree building. *Mol Biol Evol* 27:221–224. <https://doi.org/10.1093/molbev/msp259>.
  65. Zimmermann L, Stephens A, Nam S-Z, Rau D, Kübler J, Lozajic M, Gabler F, Söding J, Lupas AN, Alva V. 2018. A completely reimplemented MPI bioinformatics toolkit with a new HHpred server at its core. *J Mol Biol* 430:2237–2243. <https://doi.org/10.1016/j.jmb.2017.12.007>.
  66. Steinegger M, Söding J. 2017. MMseqs2 enables sensitive protein sequence searching for the analysis of massive data sets. *Nat Biotechnol* 35:1026–1028. <https://doi.org/10.1038/nbt.3988>.
  67. Rice P, Longden I, Bleasby A. 2000. EMBOSS: the European molecular biology open software suite. *Trends Genet* 16:276–277. [https://doi.org/10.1016/s0168-9525\(00\)02024-2](https://doi.org/10.1016/s0168-9525(00)02024-2).
  68. Söding J. 2005. Protein homology detection by HMM-HMM comparison. *Bioinformatics* 21:951–960. <https://doi.org/10.1093/bioinformatics/bti125>.
  69. Kelley LA, Mezulis S, Yates CM, Wass MN, Sternberg M. 2015. The Phyre2 web portal for protein modeling, prediction, and analysis. *Nat Protoc* 10:845–858. <https://doi.org/10.1038/nprot.2015.053>.
  70. Gao X-Y, Zhi X-Y, Li H-W, Klenk H-P, Li W-J. 2014. Comparative genomics of the bacterial genus *Streptococcus* illuminates evolutionary implications of species groups. *PLoS One* 9:e101229. <https://doi.org/10.1371/journal.pone.0101229>.
  71. Hug LA, Baker BJ, Anantharaman K, Brown CT, Probst AJ, Castelle CJ, Butterfield CN, Hershendorf AW, Amano Y, Ise K, Suzuki Y, Dudek N, Reiman DA, Finstad KM, Amundson R, Thomas BC, Banfield JF. 2016. A new view of the tree of life. *Nat Microbiol* 1:16048. <https://doi.org/10.1038/nmicrobiol.2016.48>.
  72. Facklam R. 2002. What happened to the streptococci: overview of taxonomic and nomenclature changes. *Clin Microbiol Rev* 15:613–630. <https://doi.org/10.1128/cmr.15.4.613-630.2002>.
  73. Okura M, Osaki M, Nomoto R, Arai S, Osawa R, Sekizaki T, Takamatsu D. 2016. Current taxonomical situation of *Streptococcus suis*. *Pathogens* 5:45. <https://doi.org/10.3390/pathogens5030045>.
  74. Meehan M, Lewis MJ, Byrne C, O'Hare D, Woof JM, Owen P. 2009. Localization of the equine IgG-binding domain in the fibrinogen-binding protein (FgBP) of *Streptococcus equi* subsp. *equi*. *Microbiology* 155:2583–2592. <https://doi.org/10.1099/mic.0.028845-0>.
  75. Delorenzi M, Speed T. 2002. An HMM model for coiled-coil domains and a comparison with PSSM-based predictions. *Bioinformatics* 18:617–625. <https://doi.org/10.1093/bioinformatics/18.4.617>.
  76. Smoot JC, Barbican KD, Van Gompel JJ, Smoot LM, Chaussee MS, Sylva GL, Sturdevant DE, Ricklefs SM, Porcella SF, Parkins LD, Beres SB, Campbell DS, Smith TM, Zhang Q, Kapur V, Daly JA, Veasy LG, Musser JM. 2002. Genome sequence and comparative microarray analysis of serotype M18 group A streptococcus strains associated with acute rheumatic fever outbreaks. *Proc Natl Acad Sci U S A* 99:4668–4673. <https://doi.org/10.1073/pnas.062526099>.